Preliminary study on feasibility of basaltic glass as prospective for slow fertilizer by evaluating the release rate of phosphate

Dawit Kahssay Zigta

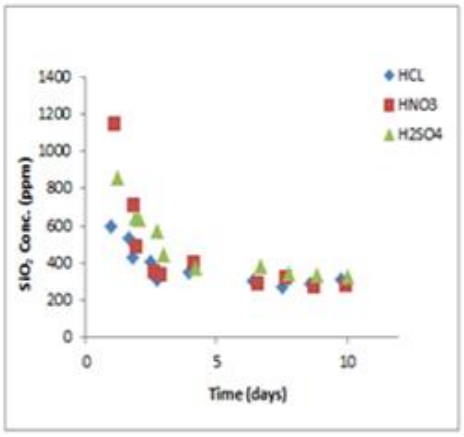

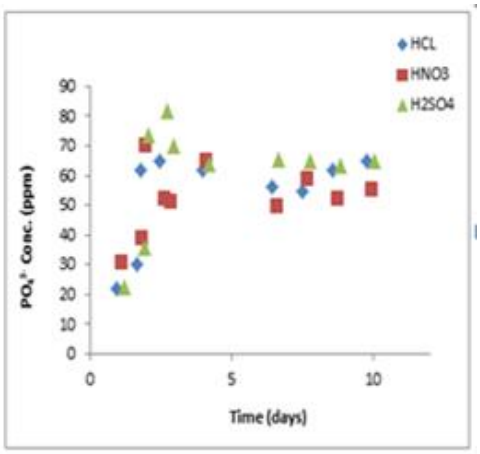

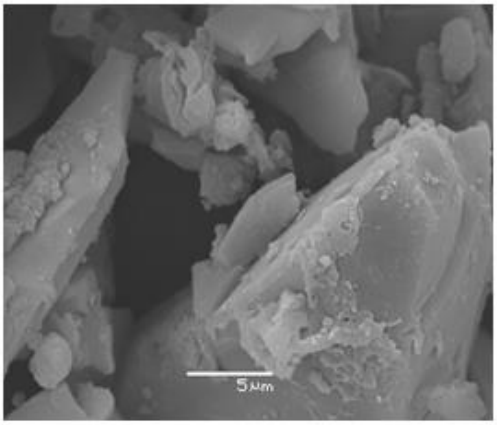

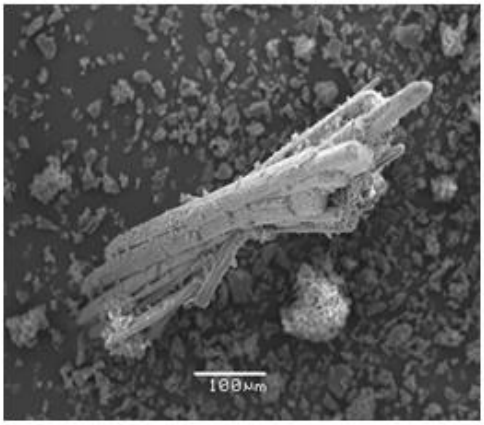

UNIVERSITY OF OSLO
FACULTY OF MATHEMATICS AND NATURAL SCIENCES

Preliminary study on feasibility of basaltic glass as prospective for slow fertilizer by evaluating the release rate of phosphate

Dawit Kahssay Zigta

Master Thesis in Geosciences

Discipline: Environmental geology and Geohazard

Department of Geosciences

Faculty of Mathematics and Natural Sciences

University of Oslo

31.03.2014

ACKNOWLEDGEMENT

First and most I would like to express my gratitude to my advisor Helge Hellevange, researcher at UiO, for his Supervision, encouragements and useful suggestions. His moral support, guidance and constructive comments were tremendous throughout the development of my thesis to the final stage. Dear Helge, I am thankful not only for the academic quality but also the dynamic and positive spirit you have.

I am also highly thankful to Beyene Girma Hailu, researcher at the University of Oslo, for his valuable support, constructive suggestions and brotherly advices. Beyene you were my courage, which this thesis wouldn't have reached here without your support.

Special thanks to Bezawit Temesgen for editing, helpful suggestions and invaluable friendly support.

I would like to express my thanks to Chemistry lab and analytical lab stuffs, Mufak Naoroz, Marteen Aerta and Berit Løken for their cooperation during my lab work.

I am indebted to thank my friends Libargachew Demlie, Teame Kiros, Shewit Kalayou as well as Minyahil Muluneh with their families. Dear friends you made my stay in Oslo pleasant without you it could have been difficult to cope with challenges of new weather and Norwegian life. I am also thankful to my friends Tewelde Tesfay and Mahamed Lamine Manga for your good friendship and valuable comments.

Mostly, I would like to give heart full thank to University of Oslo and Norwegian state educational fund (Lånekassen) for giving me this golden opportunity to carry out my study and conduct this thesis.

The last but not the least, I am highly grateful to thank my wife Hilina Debesay and my family for their invaluable support throughout my study. I would like to dedicate this work to my beloved mother Kiros Abrha. Mom I hope the heavens have all good things that I demand for you.

ABSTRACT

Improving soil fertility has been the main goal for increasing crop production in order to feed the increasing world population. Phosphorus is one of the major chemical elements commercially produced as phosphate to increase the fertility of the soil. Phosphate rock is considered the main raw material to produce phosphate type fertilizer. Looking for other viable sources of phosphorus, however, is an indispensable task in order to maximize food productivity by improving soil fertility for the increasing world population.

Hence, this study examined the potential of basaltic glass to be used as a fertilizer mainly serving as a source of phosphorus. In order to evaluate the potential of basaltic glass, the dissolution rate of basaltic glass that was obtained from Stapafell Mountain, Iceland was studied using mixed flow through reactor. The dissolution rate of basaltic glass was calculated by measuring the amount of phosphate and silica species released in the bulk solution. Ion Chromatography (IC2000) was used to determine cations and anions in the reacted bulk solution while Auto analyzer was used for measuring aqueous silica and phosphate. The solid samples, before and after reaction, were examined using Scanning Electron Microscopy (SEM). The unreacted basaltic glass and reacted basaltic glass products were also inspected using X-ray Powder Diffraction (XRD).

Matlab software program was used to simulate how the dissolution of particles of basaltic glass with different grain size distribution changes the specific surface area and hence the release rate of essential chemical species into the solution. Different values of specific kinetic rate constants, particle size distribution and time were used to simulate the optimum possible condition for dissolution of basaltic glass. The result from the first experiment shows that, the rate of dissolution of micronized basaltic glass at neutral pH and 80^0C was $1.2*10^{-9}$ $mol.m^{-2}.s^{-1}$. This dissolution rate of natural glass is too slow to release the expected amount of phosphorus (28 kg Phosphorus per hectare required for one harvest season) needed to fertilize the soil.

Hence, another experiment was performed to explore the full potential of basaltic glass. In this experiment, basaltic glass was reacted with HCl, HNO_3 and H_2SO_4.The complete dissolution of basaltic glass in acidic medium was observed. This confirms that the complete release of phosphate ion into the bulk solution from the basaltic glass structure. Treating basaltic glass with acidic solution, therefore, maximizes the release of phosphate and its feasibility to be used as a fertilizer source rock.

Pure amorphous silica was also formed as a byproduct as a result of the complete digestion of basaltic glass in acidic media as solid phase. This may open the possibility of using basaltic glass for dual purpose (fertilizer and silica source). This study shows the potential of basaltic glass as a fertilizer when it goes to complete dissolution, however additional studies should be performed in large scale to promote the use of the basaltic glass as fertilizer.

Table of Contents

Contents

Lists of Figures

List of acronyms and abbreviations

ALM – Aqueous Liquid Model

BSE – Back Scattered Electrons

CL – Cathode Luminescence

EDS – Energy Dispersive Spectroscopy

GA – Ganapathy-Anders Model

HCB – Hand crushed basaltic glass

IFA – International fertilizer industry association

IFDC – International food and agricultural development center

LS-PSA – Laser light Source Particle Size Analyzer

MiB – Micronized basaltic glass

Mt/yr – Million tons per year

P- Phosphorus

PIDS – Polarization Intensity Differential Scattering

r_{BET} – rate of dissolution based on BET surface area

SB – Synthetic basaltic glass

SE – Secondary Electrons

SEM – Scanning Electron microscope

USGS – United States Geological survey

XRD – X-ray diffraction

1. INTRODUCTION

1.1 Background of the Study

The preference of plants to grow on the weathered topsoil of volcanic terrains could imply their enrichment with nutrients that enhance their growth and production. Naturally Soil may or may not be rich in the essential nutrients for plant growth and health. Feeding the highly increasing world population had become difficult with time, though soil fertility had been treated with natural fertilizers. Therefore, increasing the agricultural production by enhancing the soil nutrition using chemical fertilizers made the modern agriculture approach paramount. This has vastly increased the use of chemical fertilizers as the main inputs to improve the crop yield from time to time (Dawson and Hilton, 2011). Hence, the current world agricultural system has become highly dependent on the availability and continued supply of different chemical fertilizers.

Phosphate, Nitrate, Potassium and sulfur are the main constituents of the modern chemical fertilizers. Relatively, the recent agricultural approach demands high use of modern chemical fertilizers than animal manure. But lack of continued supply and depletion in some of the nutrients could be the major current and future problems of the modern agricultural system (Gilbert, 2009). This can immensely increase the population suffering from lack of fertile agricultural soil, as it happened in 1850 when 1.5 billion population was threatened by lack of supply of fertilizers (Dawson and Hilton, 2011). With population estimated to increase to 9.2 billion by 2050 (Dawson and Hilton, 2011), serious consequences can be envisaged if no systems are devised to continue supply of important fertilizers.

There are no more fear of depletion for Potassium (K) and Sulfur (S) as they are sufficiently available and relatively less used as compared to Nitrogen (N) and Phosphorus (P). Hence, Nitrogen and phosphorus have been the main concerns for the last 19^{th} and 20^{th} centuries before the possibility of manufacturing ammonia was realized in the 1909 by Haber Bosch (Dawson and Hilton, 2011). Therefore, the main concern lays now days in the achievement of the demand for phosphorus fertilizer.

Phosphate fertilizers have been continuous inputs to the current farming motive and their source rocks have been mined for years in different part of the world. In 1981 the U.S has mined about 143 Mt of phosphate which was more than the world's production of salt and lime in that time (Sheldon, 1982). Sheldon has also added the consumption of phosphate was increasing at rate of 6.3% per year.

Since the use of phosphate continues increasing, it is now becoming the world's concern that the limited resource at some point will be exhausted. Numbers of studies come out with suggestion that the resource could be depleted in coming 50-100 years (Cooper et al., 2011; Cordell et al., 2009).

Limited phosphate rock resources, uncontrolled use of the fertilizer and not recycling the phosphorus rich wastes were defined as main reasons for the depletion.

Irrespective of these time limits, the world has understood that something has to be done to bring an alternative supply to this nutrient that could continue to be used in the agricultural environments so that hunger can be tackled. Could working on the geologically available phosphorus containing resources on earth be one way of sustaining the nutrient longer?

This preliminary study will focus on possible ways of enriching phosphorus from phosphate bearing inorganic reserves, such as basaltic glass. The release rate of basaltic glass was estimated using two-step experimental analyses. The first experiment assesses the natural dissolution rate of basaltic glass from which the second experiment is raised. The second experiment was on how to improve the slow dissolution of basaltic glass. Both experiments were conducted on two samples, hand crushed (HCB) and micronized (MiB). Correspondently, the result and discussion are presented in two parts. Chapter four presents results from the flow through experiment and Matlab simulation (part one) and result part two from the acid- base treatment of the basaltic glass (part two). Both results are discussed in chapter five respectively.

1.2 Statement of Problem

Soil nutrition improvement program is indisputably vital for food yields increase as well as the eradication of hunger and poverty. Yes fertilizers can improve productivity. Which fertilizer suits for which type of soil and environment, how much of which fertilizer should be used at a time, consumption rate of different fertilizers and depletion concerns have been generally discussed by some of the papers and journals referenced in this paper. Though the consumption of phosphate fertilizer has raised concern about depletion of the resource for the future use, there was no experimental work done to provide possible alternative source rocks for inorganic phosphorus. Thinking prospective for the solution, this paper focuses on slow release of phosphate fertilizers from basaltic glass that can be practiced in the current agricultural approach.

Moreover, uncontrolled application of the current phosphate fertilizers has brought environmental risks. Hence, selecting this topic was also to possibly define slow fertilizers that could be environment friendly. Therefore, utilization of natural inorganic fertilizers and their slow release not only enhance the yield but also could keep the environment less polluted. Depletion of the existing reserve, effect of high production rate, current and future demand of phosphorus was reviewed below to emphasis the concern and revel why alternative sources have to be taken into account.

1.2.1 Phosphate Rock Reserves

In the 17th and 18th centuries use of animal manure and human excreta were familiar way of upgrading the soil fertility. However, that was not sufficient to produce enough crops that could feed the continuously increasing world population, and mining of Guano was started in the mid-19th century (Cordell et al., 2009) . But this phosphate sources, Guano, were limited and at the end of 19th century phosphate rocks were discovered as unlimited resources of concentrated phosphorus (Cordell et al., 2009). Since then the demand for the phosphate fertilizer has been immensely increased and phosphate rocks are major source of phosphorus fertilizer up to now (Fig.1).

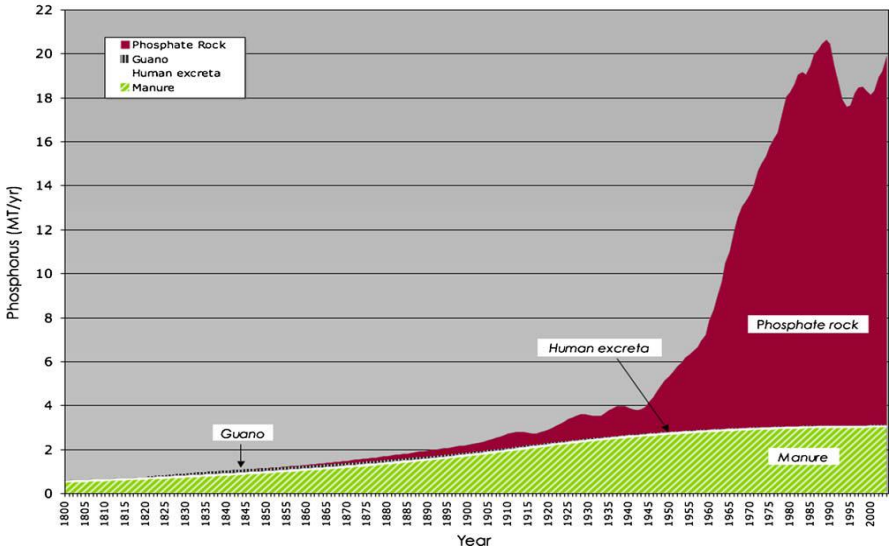

Figure 1. Shows history of world source of phosphorus fertilizer 1800-2000. Phosphate rocks were the major sources of phosphorus fertilizers. Image taken from (Cordell et al., 2009).

Analysis that apply the GA models has revealed that the earth contains $11*10^{21}$ to $13*10^{21}$ Kg of Phosphorus from the nebular condensation (Smith, 1981). According to the USGS the phosphate rock reserves are economically viable to be mined with sufficient phosphate content relative to deposition environment such as Continental shelves, sea mounts that are economically inaccessible to be mined with the current technology (Cooper et al., 2011).

1.2.2 Distribution of Phosphate Rock Reserves

The geographical occurrence of phosphate is limited with respect to temporal and spatial conditions. 77% of the global reserve is in Morocco followed by China and Algeria (Cooper et al., 2011). The US, largest consuming country, on the other hand is the seventh world reserve where its domestic reserves are left only with 25 years. The IFA and FAO report in 2006 set African as the largest exporter of high quality phosphate fertilizer and also continent with largest food shortage (IFA, 2006). This could be linked to the current price as well as global production of the phosphate fertilizer. Nevertheless, the

mining from the Western Sahara was censured by the Norwegian Support committee for Western Sahara in 2007 as it was against the international law (Cordell et al., 2009).

1.2.3 Phosphate Rock Production

The recent significant growth in agricultural yield could be linked to the rapidly increasing phosphate production. Since 1900 about 7000Mt of phosphate was produced leading to agricultural yield increase in 3.7% per year (Cooper et al., 2011). Studies and IFA reports stated annual production highly increased since 2010 and will continue to rise (Heffer and Prud'homme, 2012; Ryan et al., 2012).

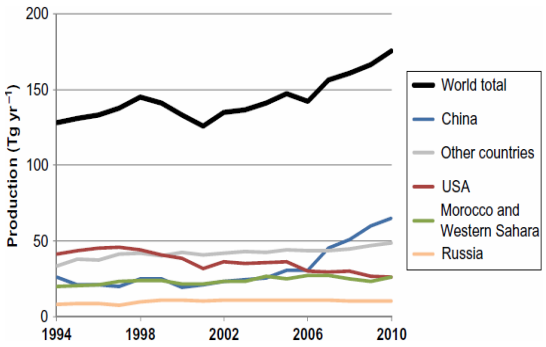

Figure 2. World phosphate rock production in 1994–2010 (USBM/USGS Mineral Commodities Summary, 1996–2011), (Ryan et al., 2012)

It seems that the geographically concentrated occurrences of the phosphate rocks give uncertainty in securing future phosphate supply. Consumption of the developed countries has raised the rate of phosphate production.

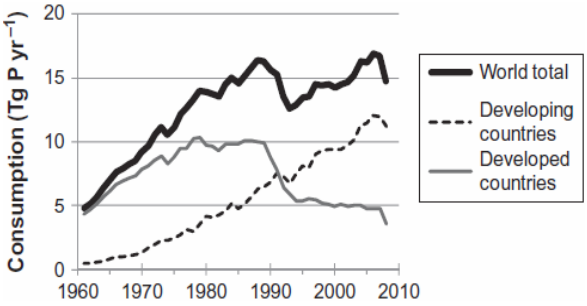

Figure 3. *Developing, developed countries and world total phosphate fertilizer consumption (Tg P yr-1) from 1961–2008 (IFADATA, 2011 recalculated from original data), (Ryan et al., 2012)*

Phosphorus was actively mined at 160 Mt/yr and no significant practical exploit was done to reduce the deficiency. Reducing rate of mining was stated as one possible way to slow the depletion (Dawson and Hilton, 2011; Suh and Yee, 2011). But this did not practiced since it couldn't provide solution to the development of food production.

The trade-wind belt-phosphates formed by the upwelling cold nutrient rich water depositing Apatite pellets, Organic rich Mud, Diatomite along the continental shelves and Equatorial group phosphate similarly formed by the east-west running trade wind were also predicted to be the future phosphate sources (Sheldon, 1982). But that did not become feasible until know.

1.2.4 Current and Future Demand

The nutrient deficient soils like that of Sub-Saharan Africa still need more application of chemical fertilizers (Figure 3). In addition, the IFDC in 2006 specified that 30% of the population in Sub-Saharan Africa applies very low fertilizer while 75% of the soil is nutrient deficient (Cordell et al., 2009). This emphasis that unlike the developed countries who have overused phosphate fertilizers, there is still very high demand for fertilizer in the developing country. The IFA indicated world phosphorus demand will show 43Mt growth in 2016 from what was in 2011(Heffer and Prud'homme, 2012) and indicated the increased by 2.9% between 2010 and 2014. Estimation of Phosphorus based on the remaining world's reserve shows, the production will decline after it reaches peak in the 2035 (Figure 4).

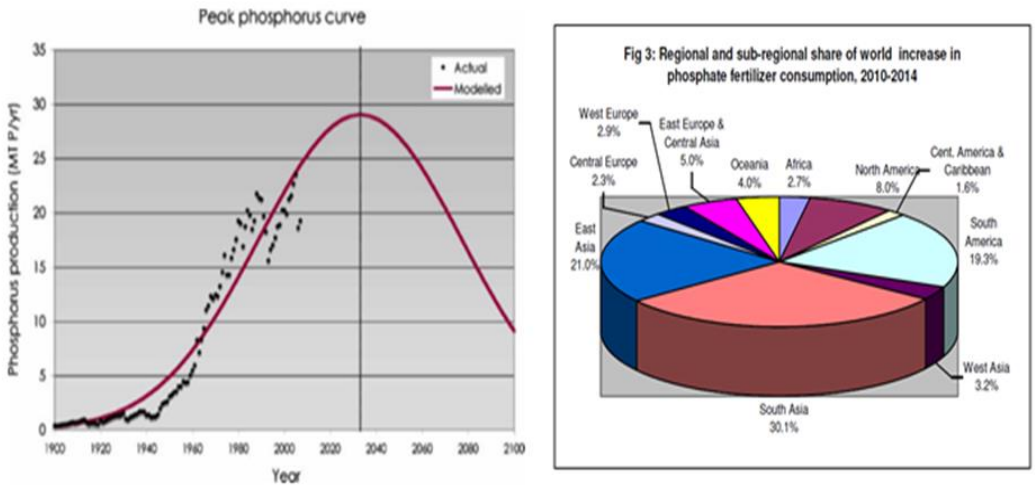

Figure 4. Illustrates the coherence of the World phosphate consumption until 2014 (right) from (Heffer and Prud'homme, 2010) and Global phosphorus production estimation and peak production curve (left) from(Cordell et al., 2009)

The current decline in phosphate reserves could cause further exploration and exploitation from available low grade reserves which defined to lack consideration of the finiteness of the resource, limited accessibility to the poor farmers and environmental contaminations (Cordell et al., 2009). Unlike that of Nitrogen, can be obtained from the air biologically and potassium, which has larger sources, phosphorus remains bottleneck for the future agricultural productivity (Hendrix, 2012).

1.3 Over Fertilization and Environmental Impact

The demand for extra production in advance by the developed countries, made the current world to apply excess phosphorus to the soil. Application of phosphorus varies from continent to continent. Europe has applied 25kg P while Africa has used 3kg P per hectare in the year 2005 (Hendrix, 2012). The application of fertilizers more than the soil retaining capacity and the crop requirement increase flow of the nutrient in to fresh water causing fast growth of plants and reduction in dissolved oxygen (Hendrix, 2012). Moreover, soil availability of phosphorus depends on the type of phosphate fertilizer applied (McDowell et al., 2003).

Mining and processing phosphorus causes adverse environmental impact in the vicinity of the mine (Hendrix, 2012) and its production from phosphate rocks involves high emission of Carbon, Radioactive elements and Heavy metal pollutants (Cordell et al., 2009).

Fluorine increased in soil threatened with phosphorus for extended period can cause fluorosis in grazing animals and drinking water (Loganathan et al., 2001). In New Zealand over-application of Cd contain phosphate affected grazing animals with kidney disease following the higher concentration of Cd in the grassland (Loganathan and Hedley, 1997).

The phosphorus concentration in runoff was high in area where the soil retaining capacity is very low. For instance, the application of the water-soluble phosphorus has cause eutrophication in the water bodies of Florida (Yang et al., 2012). This reveals that the currently applied phosphorus is not only depleting but also becoming environmentally a threat. Hence, it could be wise for the current agriculture to find a new type of phosphorus that could agriculturally effective and environment friendly.

1.4 Slow Fertilizers

Slow fertilizers have environmental and economic advantageous. These occurs as result of increase in pH and exchange of the Ca & Mg in the soil where the fertilizer rock is added (Yang et al., 2012). Many studies have been conducted on describing possible slow fertilizers.

The consistency of Phosphorus, Potassium, Calcium and Magnesium nutrients make Apatite-Biotite-Carbonatite rock more favorite to use as slow fertilizer component (Heim et al., 2012). But applying this material as fertilizer delivers the toxic elements Ba and Sr to plants as chemical weathering of the rock powder.

Dolomite phosphate rocks are also being used as slow fertilizer in areas like Florida but should be used in adjacent with commonly used Phosphorus because the phosphorus release from these rocks alone was insufficient (Chen et al., 2006).

Natural Zeolite provides mixing of Alumino-silicates with the rock phosphate, increases the dissolution due to effect of the ions exchange as well as H^+ generation through nitrification and increases plants up take of Phosphorus (Pickering et al., 2002).

Therefore, unconventional strategies such as slow release of Phosphorus have to be applied to minimize the amount of phosphorus joining the running water and partly solve the problem of water pollution. Use of slow fertilizers like Basaltic glass as source of phosphate fertilizers not only gives a handful solution to the scarcity concern of the phosphate fertilizer but also be an environmental friendly approach.

1.3 Objectives

1.3.1 Main Objective

- To evaluate the feasibility of basaltic glass to be used as source rock of inorganic phosphorus fertilizer

1.3.2 Specific Objectives

- To evaluate dissolution release rate of phosphate from basaltic glass
- To develop optimal use of naturally available resources and possibly reduce future costs of chemical fertilizers
- To assess the possibility of complete digestion of basaltic glass in acidic media to explore its potential as a fertilizer
- To determine the solid mineral phase that may be form during acid digestion of basaltic glass

1.4 Limitation of the study

The limitations here could be technical, like the accuracy of the computations resulted from assumptions regarding the real natural system. The impractical to use the ICP-MS equipment after long waiting resulted shortage of time and may present impact on the quality of the output data. Concentration of Aluminum was not measured due to safety reason for the analytical equipment. In the natural environment, weathering of the rocks could be controlled by physical and chemical processes. It is clear experimental analysis have made the complex nature simple and understandable. However, dissolution rate parameters used in this study are approximations of their true field situations. Such as geometric surface area of grains were calculated assuming all particles

spherical. It also was stated actual geometric surface area might be orders of magnitude less than estimated physical surface area (Rowe Jr and Brantley, 1993). Hence, interpretations have to be based on their assumptions and consideration of the numerous processes (such as geological and hydrogeological interactions). Combined evaluation of the effects of change in particle distribution, prevailing temperature, pH and hydrological character of the different soil types as well as late formed secondary layers might provide better result.

1.5 Outline of the Study

The thesis has six chapters. Short outline of each chapter follows:

1. Introduction: introduces the general background of the thesis, the statement of the problem, main and specific objectives and outline of the thesis. The fertilization and status of phosphate fertilizer, problem the thesis addresses and purpose of the study were dealt in this chapter.

2. Theoretical background: this chapter reviews the previous works on the occurrence and dissolution rate of basaltic glass. It also presents occurrence of phosphate, speciation of phosphate with pH as well as why basaltic glass was chosen as possible source rock of phosphorus.

3. Experimental system: this chapter is concerned about laboratory experiments and analytical methods used to collect data. Procedures followed to conduct the mixed flow experiment and analyze the aqueous and solid samples were discussed. Softwares used for modeling were also described.

4. Results: results from both experiments and Matlab and Preeqc simulations output are presented in this part. Rate of dissolution for the basaltic glass, released rate of ions as function of time, complete extraction of phosphorus as result of acid treatment and mass of basaltic glass required to convey the recommended amount of phosphorus per hectare are determined.

5. Discussion: in this part of the thesis the experimental and simulation results are discussed briefly. Feasibility of basaltic glass as source rock is clarified.

6. **Conclusion and recommendation**: Presents the conclusion reached through the study and finally future researches are recommended.

References: presents list of bibliographies and authorities used in this research.

Appendixes: this part contains brief details of mass calculation, tabulated results and derivation of formulas used to set experimental procedure as well as in the result and discussions.

2. THEORETICAL BACKGROUND

2.1 Occurrence and abundance of Basaltic glass

A study by (Morgan and Spera, 2001) stated rapid cooling of magma on the earth produces about one billion km^3 glass, which most of it is basaltic glass. Volcanic glass was rated as the third abundant rock on the continental crust covering about 12% of the surface (Nesbitt and Young, 1984). Potential deposits of basaltic glass were stated to occur along Oceanic islands, Island arcs (of Hawaii, southern and Western Samoa), active divergent plate tectonics (African rift valley) and the 70, 000km glob-encircling ridge such as volcanic province of Pacific Ocean (Morgan and Spera, 2001; Smith et al., 1978).

2.2 Basaltic glass dissolution and controlling factors

In addition to its abundance, the fast reactivity of basaltic glass was said to contribute numerous metal oxides, silicate and phosphorus oxide to nearby environment. Moreover, low alteration temperature in the seafloor and higher hydraulic conductivity in the glassy surface were other specified reasons for the high degree of weathering in addition to the non-crystalize structure (Gislason and Oelkers, 2003).

Another study stated Stoichiometric dissolution of basaltic glass take longer time not only in the neutral condition but also last several hours in acidic and alkaline condition (Guy and Schott, 1989). The reason was that the destruction of the tetrahedral coordinated inner layer composed of Si, Al and Fe (III) is durable.

Similarly, (Oelkers and Gislason, 2001) have stated far from equilibrium dissolution of basaltic glass is dependent to the concentration of aqueous aluminum in both basic and acidic conditions. The collective emphasis by these studies would imply removal of adjacent aqueous Al could enhance the breaking of the bond and reduce Si replacement in the glass structure and possible sorption.

Oelkers and Gislason added the dissolution of basaltic glass is proportional to the concentration of partially detached silicon tetrahedral at the surface of grains (Oelkers and Gislason, 2001).

Experimental study on behavior of trace elements Li and Cs, during the dissolution of basalt indicates the destruction of the host silicates will convincingly move the trace elements in to the solution or the solid phases (Berger et al., 1988). It shows the separating of Li and Cs in to hydrothermal minerals, chlorites and smectite as well as preferential leaching of Cs and stoichiometric release of Li with respect to silica.

A study by (Harley and Gilkes, 2000) explain their doubt in the feasibility and effectiveness of the different silicate source rock prospects for inorganic fertilizer. The low solubility of silicate rocks, distribution and solubility of nutrients in the rock as well as mineral weathering rates were identified factors that cause time bound infeasibility of using the different inorganic fertilizers source rocks.

2.2.1 Surface area and grain size

The specific surface area is determined by the distribution of the grain sizes, which indirectly means the grain size distribution controls the kinetics of the dissolution of the basalt glass.

Basaltic glass dissolution was studied as function of its composition where the effect of BET and Geometric surface area on the rate was compared(Wolff-Boenisch et al., 2004b). They found that the r_{BET} was smaller due to coating on the surface of grains. As atoms are detached from the surface of the grains the rate is proportional to the aqueous surface area.

Berger et al. studied dissolution of basaltic glass at 200^0C in sea water to verify whether the surface area or later developed coating layers control the reaction (Berger et al., 1987). They found selective removal of species, which implies formation of diffusion prohibiting surfaces (e.g. smectite) control the alteration but not surface reaction.

Another study on far from equilibrium dissolution rate at 25^0C temperature and pH < 11 indicated the dissolution rate is pH and Surface area dependent at lower pH but at higher pH it becomes pH independent (Helgeson et al., 1984)

2.2.2 Time

Chemical reactions and rate of removal of elements/ions in nature take place as function of time. The unit of the rate depends on the definition of the reaction and could be $mol.m^2.s^{-1}$ or $mol.s^{-1}$ (Appelo and Postma, 2005). Generally rate is expressed by the change in concentration with time.

$$r = -\frac{dC_i}{dt} \text{---------- 2.1}$$

The negative sign implies the rate is a decreasing rate. Field weathering rate of minerals with difference in relative strength was stated by Samuel Goldich in 1938. Though recent advance in laboratory rate measurements allowed prediction of natural weathering rates, discrepancies may occur as they represent different time duration and actual physical conditions. It looks why (White and Brantley, 2003) produced a general rate expression for decreasing silicate weathering with time at ambient temperature ($r = a * t^b$; a is intercept and b the slope of regression line).

2.2.3 Fluoride and environment

Aqueous Fluoride has a positive effect in enhancing the dissolution of basalt glass. The formation of aqueous aluminum fluoride complexes limits the activity of Al^{+3} which is a limiting factor in calculating the far from equilibrium rate of glass dissolution (Wolff-Boenisch et al., 2004a).

$$\log r = \log k + \mathrm{n}.\log(\frac{a_H^+}{a_{Al}^{+3}}) \quad \text{2.2}$$

Where k is specific rate constant, n stoichiometric constant and a activity of the subscript species.

Figure 5 shows speciation of aluminum in acidic aqueous medium as a function of fluoride ion. At fixed pH 4 and temperature of 25 ^{0}C, the activity of aluminum ion decreases due to the affinity of Aluminum to form complexes with fluoride ion following the increase in fluoride concentration.

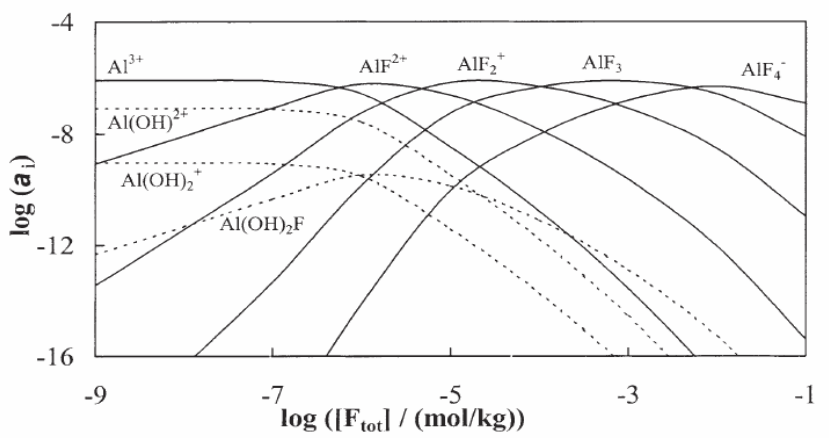

Figure 5. Computed activity of Aluminum as a function of total fluoride concentration at pH 4 and 25^{0}C for a total Al concentration of 10^{-6} mol/kg (Wolff-Boenisch et al., 2004a)

Similarly, another study showed that solubility of Fluorine is higher at acidic due to forming complexes with Al (Mezghani et al., 2005). It also added displacement of F^- by OH^- might increases fluorine release at alkaline pH.

Though phosphate rocks are the main source of Fluorine in pastoral soils, the concentration of fluorine in Phosphate rocks especially in fluorapatite was defined very low (Loganathan et al., 2008). In addition, recent recommended application of phosphate fertilizers to moderate acidic soil made it unlikely to increase the Al-F complex to cause photo-toxicity (Manoharan et al., 2007). But environment health and safety guideline report has identified HF, SiF_4 which are the byproduct of current phosphate fertilizer manufacturing system should be determined for environmental purpose (EHS, 2007). This also provides possible implication that use of slow release fertilizers would reduce the concern much better than the current sedimentary derived phosphate fertilizers.

2.3 Occurrence of Phosphorus

By nature some elements are inert while some are highly reactive and are only found in compounds. Phosphorus is reactive element that does not occur as free element in the earth and apatite seems the principal storage major storage. Microprobe analysis on tholeiitic basalt from the upper mantle revealed the Apatite contains 18 wt% of P (Smith, 1981). Smith added, Phosphorus ranked as the eleventh abundant element in the earth crust occurred 95% as Apatite and the earth's crust accounts an average of $8*10^{8}$ million tons of phosphorus.

2.4 Chemistry of phosphorus in aqueous solution

Inherently soils are deficient in phosphorus content to enhance crop production that enables feeding the continuously growing population. Hence, application of P fertilizer has become the ultimate choice.

A study defines that fertilizer application increases total inorganic phosphorus in the upper 15 cm soil decreases with depth (Takahashi and Anwar, 2007).

Experiment on crop responses to applied phosphorus concentration has revealed for groundnut 20 kg P and wheat 40kg P per hectare is adequate (Aulakh et al., 2003). A similar study determined recommended phosphorus concentration to be 23-28kg P per hectare (Ross H., 2013).

Another study on plant available P expresses it is difficult to exactly determine the concentration of plant available P in different soils because of different mechanisms that affect the environmental availability of phosphorus (Devau et al., 2009).

Phosphorus occurs in different forms such as in mineral, particulate and dissolved form in the earth. Orthophosphates or p (-III) compounds are the most know plant available forms of phosphates (Hanrahan et al., 2005). However, the distribution of phosphorus compounds in the environment significantly affects the bioavailability of these species to plants.

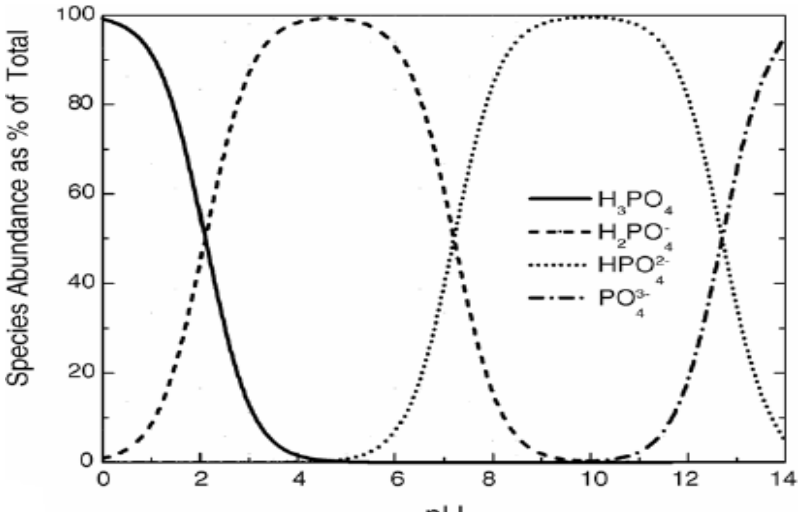

Figure 6. Speciation of phosphate as function of pH based on the pKa values, pKa_1=2.1, pKa_2=7.2 and pKa_3=12.7 from (Hanrahan et al., 2005).

The speciation of P with change in the pH indicates the $H_2PO_4^-$ and HPO_4^{2-} ions are dominant species in the circum-neutral pH. In line with this, (Gustafsson et al., 2012) stated the pH of agricultural soil fluctuates due to harvesting as well as liming practice, which in turn affect the solubility and sorption of the phosphorus species accordingly. Moreover, the redox condition will determine which oxides or hydroxides of Fe (III) and Al are the sorbents.

2.5 Why basaltic glass and why phosphorus

The abundance on the ocean floor as well as in volcanic terrains and its relative rapid dissolution rate are not the only reason that basaltic glass can be used as prospect for slow fertilizer. The environmental benefits it can provide are also additional merits beside of being the source of numerous metals and nutrients. Scientist in the Norwegian University of Life Sciences (NMBU), have come out with a study to reduce the emission of N_2O and CO_2 from agricultural soil by applying non-carbonate materials to raise the pH of the earth which agrees with the scope of this paper (www.geoforskning.no).

They have indicated that minerals have the effect of buffering the pH of the soil without emitting CO_2 and consequently reduce the emission of N_2O. Moreover, the slow release of inorganic phosphorus can also reduce the Eutrophication problem raised now days due to the chemical phosphorus applied in agricultures.

Furthermore, the application of basaltic glass fertilizer could enhance the cation exchange capacity and acid neutralizing capacity of poor soil, which (Harley and Gilkes, 2000) express for possible silicate slow fertilizers.

High P content of Mantle silicate was studied partitioning in to phosphorus distribution between clinopyroxene, olivine and glass where glass has 0.75 -1.3 wt % Phosphorus. That is higher phosphorus content than Olivine 0.07 – 0.15 wt%, Amphibole 0.035 – 0.07 wt% and Clinopyroxene 0.015 – 0. 06 wt% (Brunet and Chazot, 2001).

The over-application of P emphasis its agronomic efficiency is greater than N and K Particularly with plants growth. The fertilizer dependency of the current agricultural practice, the intensive application of Phosphate fertilizers and depletion of the resources are the motives in addition to the environmental disruption (eutrophication).

3. EXPERIMENTAL SYSTEM

3.1 Introduction

Mixed flow experiment was conducted on Basaltic glass collected from Stapafell Mountain, Iceland. Collected fluid samples were chemically analyzed. The basaltic glass chemical formula, $SiAl_{0.365}Fe_{0.191}Mn_{0.003}Mg_{0.294}Ca_{0.263}Na_{0.081}K_{0.008}Ti_{0.025}P_{0.004}O_{3.405}$, was obtained from Stockmann. (Stockmann et al., 2011).

3.2 Characterization of initial material

Prior to flow through experiments, initial sample material was characterized using XRD and SEM. XRD spectrometry explains 85% of the sample was non-crystalline/glass and the remaining 15% crystalline. The crystalline minerals found in this sample are mainly Forsterite and some Quartz

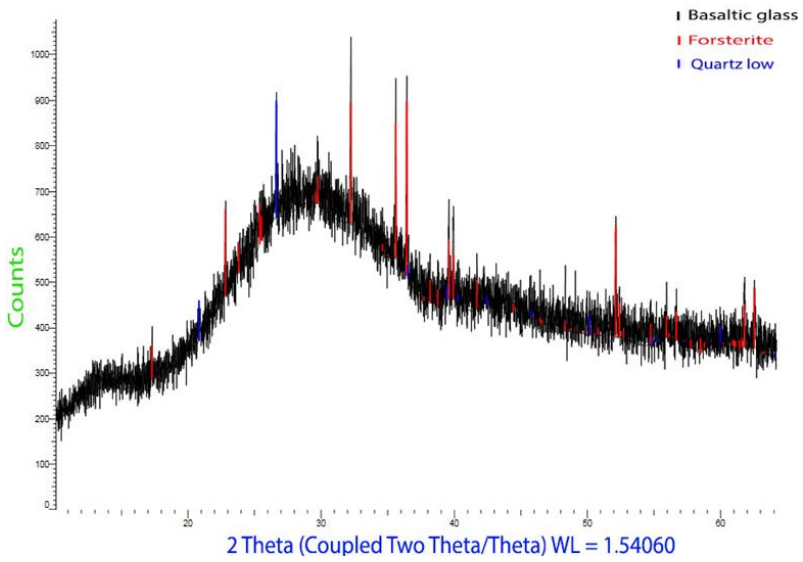

Figure 7. XRD analysis spectrum of unreacted basaltic glass

Thin gold coated representative grains of HCB and MiB were analyzed using low voltage SEM. Rough grain size distribution estimation; surficial impurities and detail surficial structures were studied using same EM image with different magnification (Fig. 8).

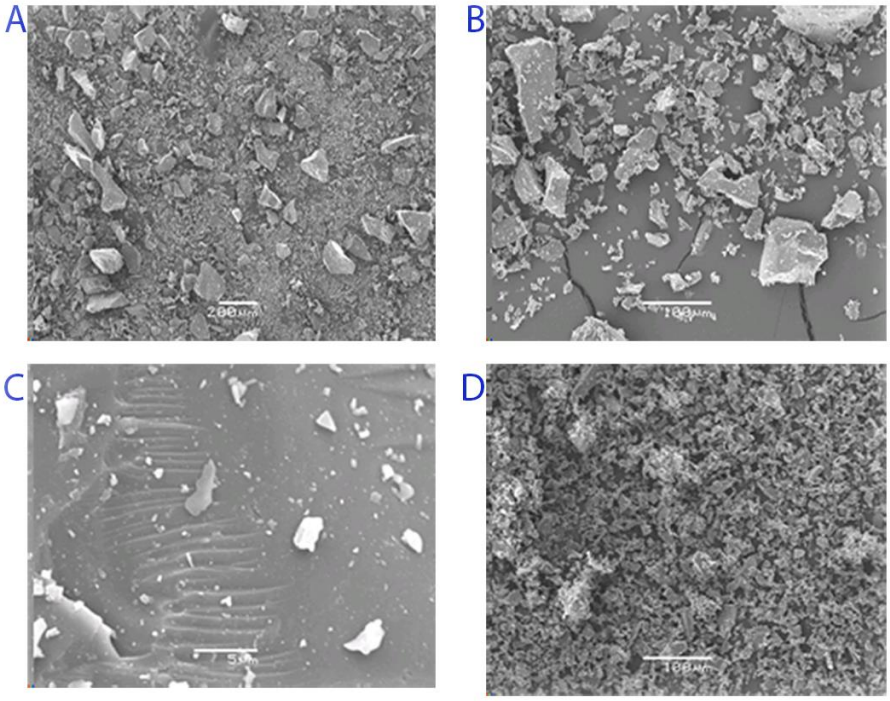

Figure 8. SEM analysis of unreacted basaltic glass A) bimodal 90% fine grained HCB B) Three size families HCB with 75% fine grained, C) HCB used for grain surface Impurity check , D) Micronized

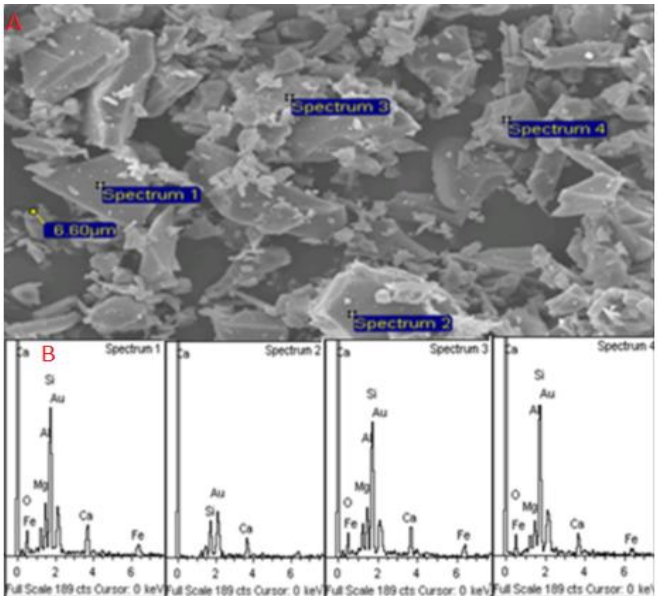

Figure 9. SEM/EDS analysis of unreacted basaltic glass A. spots at which grains were selected for elemental analysis and grains size measurement B. spectrum showing Elemental composition of the different grains analyzed under SEM/ EDS. The Au in the spectrum is from the coating

3.3 Experimental Procedures

Descriptions of the procedures are presented in two parts. The first experiment includes crushing, particle size analysis and flow through experiment. The second part was started after completion of experiment one and in this phase basaltic glass was treated with acid and base.

3.3.1 Method for Experiment One

3.3.1.1 Crushing

49.8g of basaltic glass (labeled HCB) was manually crushed using agate mortar and pestle and 52.3g of the basaltic glass (labeled MiB) was pulverized to a grain size of <0.2mm electronically using micronize machine. For SEM, PSA and dissolution rate experiments the whole 49.8g of the HCB and 50.3g of the MiB were used. The remaining 2g of the MiB was used for XRD analysis. Ethanol was added to the glass to minimize loss of grains during crushing and make crushing easier.

3.3.1.2 Particle size distribution Analysis

Grain size distribution analysis was carried out using the Beckman coulter LS 13 320 Particle Size Analyzer (LS-PSA). A sonic stirrer was used to mix, separate the solution and pick representative sample. 532 mg of sample was taken from each of the samples and diluted with Sodium Meta-phosphate (NaO_3P) to disperse the grains. Result is displayed (Table 2, Appendix I) as volume % in discrete size classes. Geometrical specific surface area (s_{Geo} in $m^2.g^{-1}$) was calculated using eq. 3.1 based on the data obtained from LS- PSA (detail steps Appendix I, C).

$$s_{Geo} = \frac{3}{\rho}\sum_i \frac{x_i}{r} \quad \text{..... (3.1)}$$

Where X_i is volume fraction of basaltic glass, i discrete size classes, ρ density of basaltic glass (2.9g/cm^3) and *r* radius of grains respectively. The calculation of the surface area from the grain size considers all grains as spherical. The surface area used throughout this study was geometric surface area. Illustration of the particle size analysis is given below. Range of particle size distribution for the hand crushed (HCB) & micronized (MiB), differential and cumulative volume % as well as computed (s_{Geo}) and analytical (differential &Cumulative) surface areas are demonstrated from figure 10 –15.

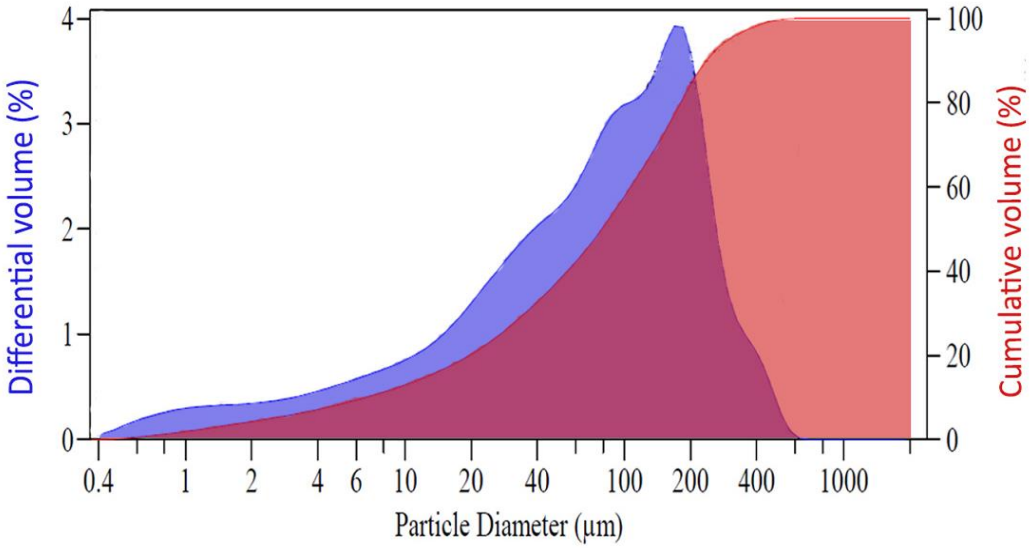

Figure 10. Change in the differential and cumulative volume (%) with respect to grain size (µm) for HCB ; the high volume of particle size range is between 100µm -200µm that is 10 time larger than micronized.

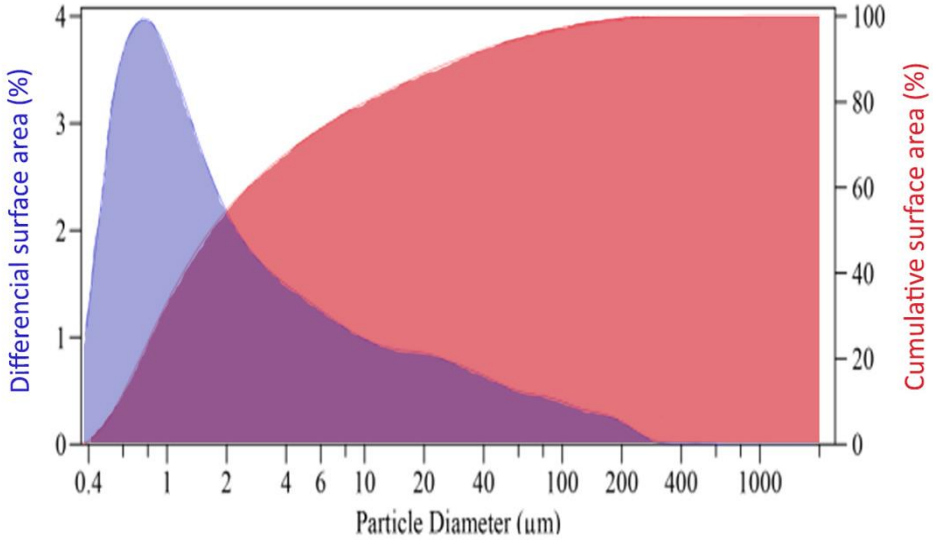

Figure 11. Expression of the variation in Experimental cumulative and differential surface area (%)with grain size for HCB. the analithical statistics also revels particle sizes <7.776µm make 80% of the surface area(%).

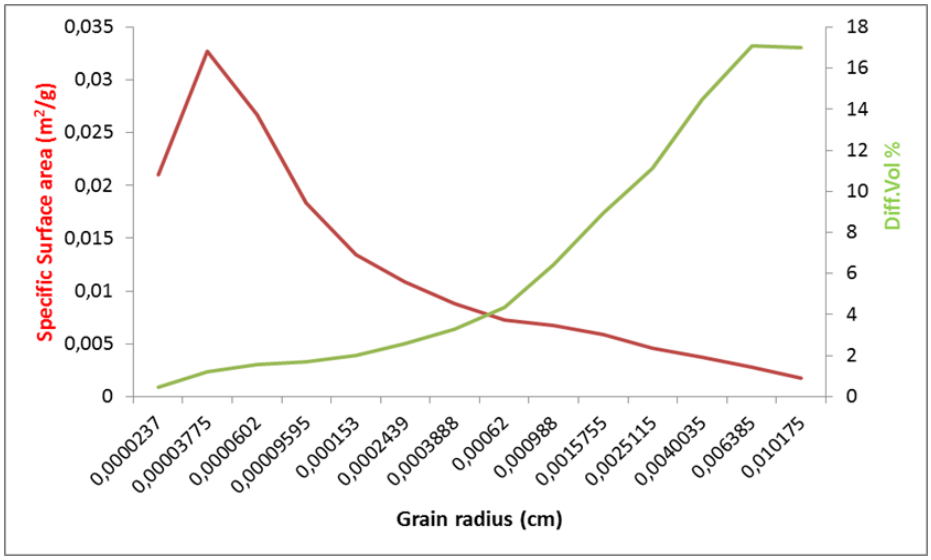

Figure 12. Illustrates the change in specific surface area ($m^2.g^{-1}$) and differential volume (%) with particle size, HCB. The calculation of the Surface area from the grain size considers all grains as spherical.

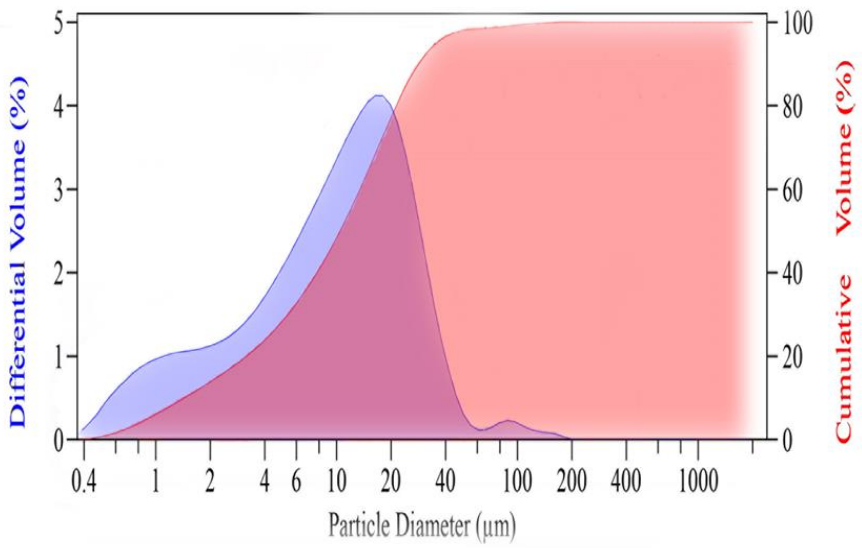

Figure 13. Experimental result showing change in the Differential and Cumulative volume (%) with respect to grain size (µm), MiB; the high volume of particle size range is 10 µm -20µm which is 10 times lower than hand crushed sample.

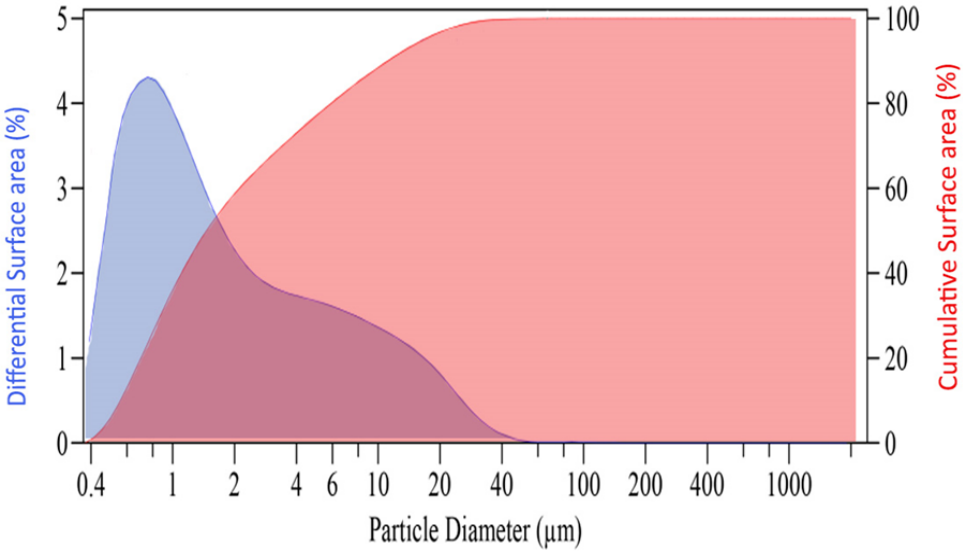

Figure 14. Expression of the variation in Experimental cumulative and differential surface area (%)with grain size for MiB . the analithical statistics also shows particle sizes <4.6µm make 80% of the surface area(%).

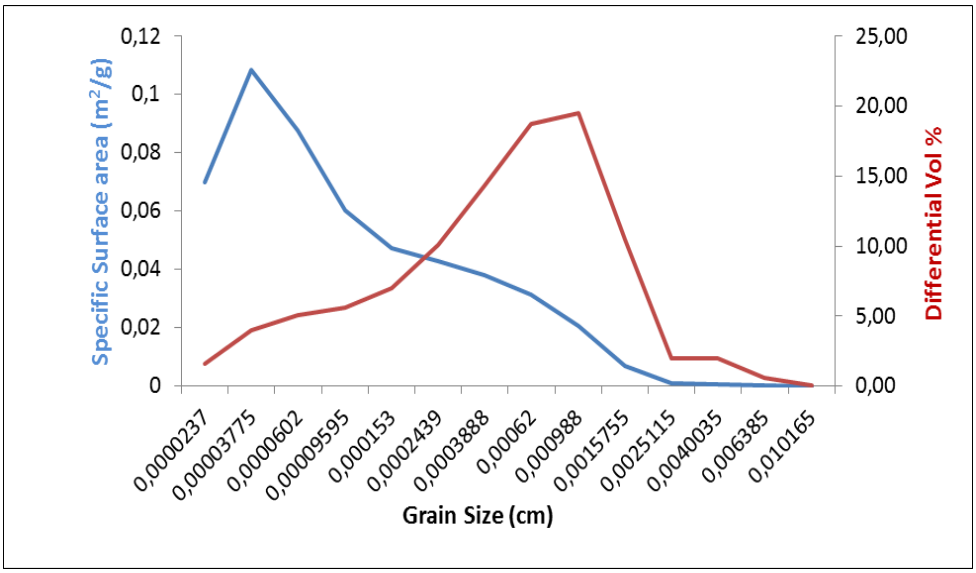

Figure 15. Illustrates the change in the calculated specific surface area and differential volume % with particle size, MiB.

The above illustrations showed the change in differential surface area (analytical output) and calculated geometrical surface area as a function of the particle size for both samples were similar. Mixed flow experiment was chosen because of its flexibility and closer analogous to weathering in a natural regoliths (allow infiltrating water progressive reaction with a continuum of mineral phases). Non-stirred 250 ml polypropylene reactors were placed in a shaker bath at a temperature of 80°C and pH 7. Two reservoirs were filled each with 800 ml distilled water, 20g HCB and 10g MiB basaltic glass were added respectively to the two reactors. A peristaltic pump was used to flow water in the

reservoirs to the reactors through tubes and drive aqueous solutions from the reactors. The discharge through the tubes was collected in to bottles three times a day (Appendix I, A) and chemically analyzed using Ion chromatography and Colorimeter. The dried solid samples were analyzed under SEM to determine surface coating and secondary minerals formation. The rate of dissolution (r) was calculated by;

$$r = \frac{Q*\Delta C_i}{S*n_i} \quad \text{.....3.2}$$

Where Q is flow rate ($g.s^{-1}$), Δc_i is difference between individual inlet and outlet concentrations ($mol.g^{-1}$), S is the surface area of reaction (m^2) and n_i is stoichiometric coefficient of element i in the glass.

Before starting the experiment a literature review of glass dissolution rate was done. The rate as function of pH was recalculated according to (Gudbrandsson et al., 2008) as shown in figure 16. These rates were used to adjust the flow rates (Q) that possibly prevent precipitation of silica (amorphous or microcrystalline). Calculation details can be found in Appendix I, B.

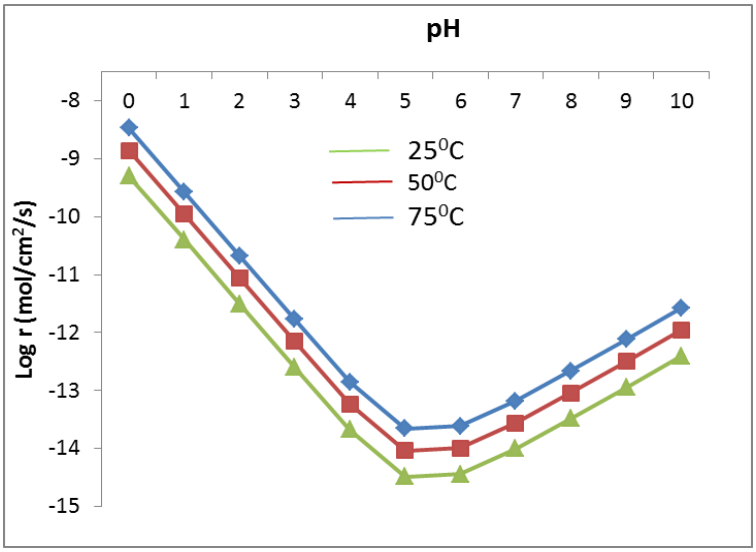

Figure 16. Characterization of rate of release as function of pH at 25^0C (green), 50^0C (red) and 75^0C (blue); activation energy was used from (Gudbrandsson et al., 2008)

The mole of basaltic glass required to dissolve the Concentration of Phosphorus per hectare per year was calculated using e.q.3.3.

$$n_b = \frac{C_P}{x_p^b\,(1-exp^{-(k**s*M_b*t)}} \quad \text{.....3.3}$$

Where n_b is moles of basalt, C_p is amount of phosphorus per hectare per year, X_p is fractions of phosphorus in 1 mole of basaltic glass (g), k is specific rate constant ($mol.m^{-2}.s^{-1}$), s is specific area

($m^2.g^{-1}$) and t is time (sec). Consequently, the mass of basaltic glass was also calculated based on the result from eq. 3.3 (calculation details Appendix II).

3.3.2 Method for Experiment Two

As will be presented in the result part one of chapter 4, the result from the first experiment showed the rate at which silica and phosphorus released was very slow. This raised query of separating Phosphorus from the framework of the glass. Hence, pretreating the basaltic glass with acid and /or base might generate a material with more phosphorus and high reactivity.

Therefore, in this second experiment the basaltic glass was pretreated separately with HCl, HNO_3 and H_2SO_4 acids. 5g of basaltic glass was diluted with respective concentration of each of the acids at pH zero and placed in a heating bath (JB Aqua 26 plus) at 90^0C for 15 days. The same procedure was used to prepare the solution for each of the acids as the procedure for sulfuric acid, given below.

5g of basaltic glass was diluted with 0.5M (1N) of concentrated sulfuric acid. The final volume of the solution was 300 ml for all three reactors. The volume of sulfuric acid to be diluted was calculated for 1N (equivalent for 1mole of H^+), which is 0.5M of H_2SO_4, for comparison with the other two acids. Eq. 3.4 was used to calculate the volume of each of the acids needed to prepare the total solution.

$$M_1 * V_1 = M_2 * V_2 \quad \ldots\ldots\ldots\ldots\ldots\ldots\ldots\ldots \quad 3.4$$

M_1 and M_2 represent initial and final molarity ($mol.l^{-1}$), V1 and V2 stands for initial and final volume (ml) used to prepare 1N solution of the acids respectively. Accordingly, the volume of sulfuric acid required to produce 300ml of reactor is 8.4ml. HCl was chosen to favor non-oxidizing acid and weak reducing property while HNO3 is an oxidizing acid. 1 M was used separately for both of these acids. The volume required to prepare the 300ml solution was 24.7ml of HCl and 20.92 ml of HNO_3. The pH of solution measured after the distilled water and the acids were mixed was 0.19, 0.13 and 0.11 for H_2SO_4, HCl and HNO_3 respectively.

Total of 10 liquid samples were collected including the bulk solution sample in 15 days. The solid material was placed on a filter paper in a sucking pump and rinsed using distilled water.

Basaltic glass of 20.5 g was reacted with NaOH at 90 ^{0}C and pH 12.5 in another experiment to compare with digestion reactions of basaltic glass in acidic media. This will be presented in chapter five part two.

3.4 Analytical Methods

3.4.1 Ion Chromatography (IC)

10 sample tubes for each of the HCB and MiB containing 6ml of liquid samples were loaded on the automated sampler. The ICS 1000 and ICS 2000 were used to measure cation and anion concentration respectively. Ion Pac CS16 column separates cations sequentially based on their charge and mass size while the anions were separated based on Ion exchange (in accordance to their interaction with the exchange sites) using Ion Pac AS18 column. A chromatogram is produced from the detected electric conductance of each ion measured by the detector. The peak heights were quantified by chromeleon and converted to concentrations in relative to the standard.

3.4.2 Colorimetric (CM)

The concentration of Silica and PO_4^{-3} in the sampled solution was determined using the AA3 (Auto analyzer) colorimeter. Standard solutions were prepared for every analysis conducted. Aqueous standard was prepared using 15g Ascorbic acid, 2g Sodium dodecyl sulfate and 4.4g potassium dihydrogen phosphate each diluted by 1000ml DI water. AA3 method number G-103-93 was used to determine the concentration of phosphate as the orthophosphate reacts with molybdate and ascorbic acid. Aqueous standard solution for the silica analysis was prepared from 6.82g ammonium molybdate, 59.3g Oxalic acid, 1g sodium dodecyl sulphate and 4.73g of sodium metasilicate nonahydrate each separately diluted in 1000ml Di water. The AA3 method applied was G-147-95.

3.5 Statistical and Graphical Methods

The likelihood of super saturating some of the phosphate minerals as a function of reaction progress was simulated using Phreeqc. NaOH were reacted with aqueous solutions that contain the metal cations and orthophosphate ions to neutralize the acid and super saturate phosphate minerals at 25 ^{0}C, 90 ^{0}C and pH 1. Concentrations from analytical results were used to define the composition of the initial solution in Phreeqc. Input concentrations were in ppm. The key word REACTION was used to define reaction steps and stoichiometric formula of Sodium hydroxide (reactant). Data files were produced using the Keyword SELECTED_OUTPUT data block.

Matlab was used to explore how preferential dissolution of fine particles affected the specific surface area and release rate. The different values of specific rate constants, particles diameter and durations were simulated using a specific model developed by Helge Hellevang in matlab program. Graphs were customized using Photoshop and Microsoft Excel. Excel spreadsheet was used to create table for the experimental and calculation data.

4. RESULTS OF RATE EXPERIMENTS

The results from the study are presented in two parts. Results presented in part one defines the outcomes of the first flow through experiment as well as results from Matlab simulation and result in part two refers to the results of the second experiment on both micronized and hand crushed samples.

4.1 Result Part One

The flow through experiment was conducted at pH 7 and 80^0C and liquid samples were collected for both hand crushed (HCB) and micronized (MiB). Analytical results are given in Table 4.1 and 4.2. The values of nitrate and phosphate ions for some samples labeled as n.a. (no analytical result) are due to their lower concentrations compared to the detection limit of the IC.

Table 4.1 Concentrations of ions in the reacted bulk solution for the reacted hand crushed basaltic glass

Sample	**Amount in mmol.l^{-1}**								**Sampling time**
name	**F**	**NO_3**	**SO_4**	**PO_4**	**K**	**Mg**	**Ca**	**Si**	**days**
R4 1	0,013	0,007	0,037	0,0041	0,059	0,077	0,115	0,187	0,21
R4 2	0,003	n.a.	0,004	n.a.	0,007	0,022	0,034	0,044	0,84
R4 3	0,004	n.a.	0,004	n.a.	0,009	0,039	0,059	0,087	0,99
R4 4	0,009	n.a.	0,004	n.a.	0,014	0,041	0,064	0,094	1,15
R4 5	0,005	n.a.	0,005	0,0042	0,013	0,065	0,123	0,199	1,83
R4 6	0,005	0,006	0,004	0,0040	0,010	0,037	0,077	0,105	2,02
R4 7	0,004	n.a.	0,004	0,0041	0,008	0,039	0,090	0,117	2,16
R4 8	0,004	n.a.	0,004	n.a.	0,008	0,030	0,065	0,083	2,92
R4 9	0,004	n.a.	0,004	n.a.	0,007	0,029	0,062	0,089	3,11

Table 4.2 concentrations of ions in the reacted bulk solution for the reacted micronized basaltic glass

Sample name	Amount in mmol.l-1								Sampling time
	F	NO_3	SO_4	PO_4	K	Mg	Ca	Si	days
R5 1	0,013	0,007	0,031	0,004	0,016	0,066	0,101	0,474	0,21
R5 2	0,005	0,007	0,008	0,004	0,012	0,050	0,098	0,340	0,88
R5 3	0,004	n.a.	0,004	n.a.	0,009	0,047	0,092	0,274	1,05
R5 4	0,004	n.a.	0,004	n.a.	0,008	0,046	0,090	0,248	1,22
R5 5	0,004	n.a.	0,003	n.a.	0,007	0,036	0,075	0,178	1,89
R5 6	0,005	n.a.	0,004	0,004	0,009	0,041	0,092	0,197	2,06
R5 7	0,004	n.a.	0,003	0,004	0,008	0,034	0,070	0,182	2,23
R5 8	0,004	n.a.	0,005	0,005	0,013	0,034	0,182	0,358	2,99
R5 9	0,003	0,006	0,005	0,004	0,008	0,025	0,103	0,151	3,18

Figures 17 to 23 illustrate the change in released concentration of ions as a function of time in consensus to equation 2.3. This temporal evaluation of release rate of each ion suggested that a steady state was attained between first and second days.

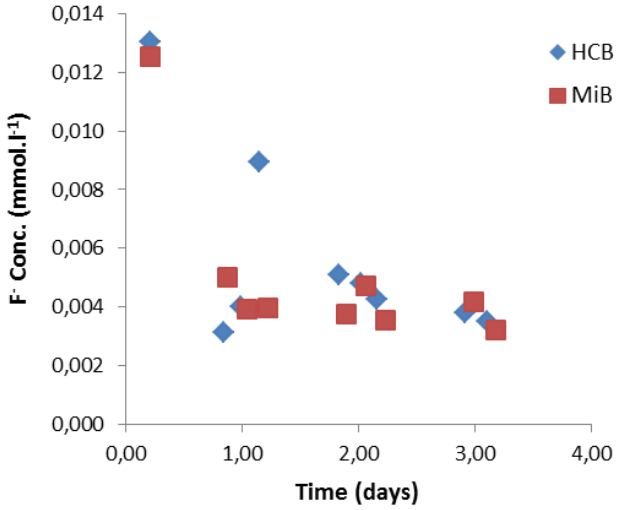

Figure 17. Concentration evolution for fluorine ion as function of time for both samples

Decreasing release rate of fluorine reaches to a steady release rate at day one (Fig. 17).

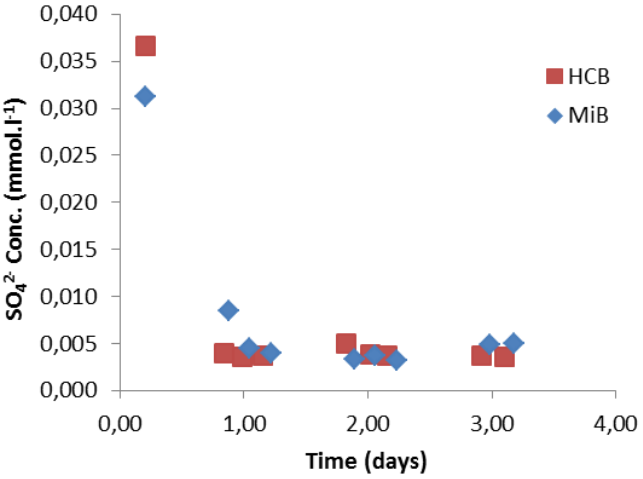

Figure 18. Concentration evolution for Sulphate ion as function of time for both samples

Release of sulphate from both samples display a sharp drop and reach steady release after day one. The release rate of sulphate ion is consistent for both samples relative to other anions.

The release of Phosphate from both samples looks steady except the increase from micronized sample to 0.051 mmol.l^{-1} at third day. There is missing data in the plot from 0.5 to 2nd day that displays the concentration below standard.

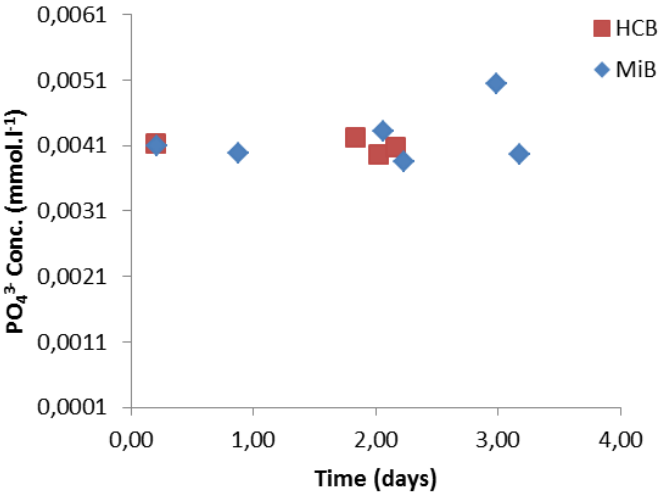

Figure 19. Concentration evolution for phosphate as function of time

The release rate of cations from HCB in general showed gradually decreasing release rate with time (Figures 20 - 23). Relatively K^+ showed consistent release from both samples and it looks that steady state release was attained after day one.

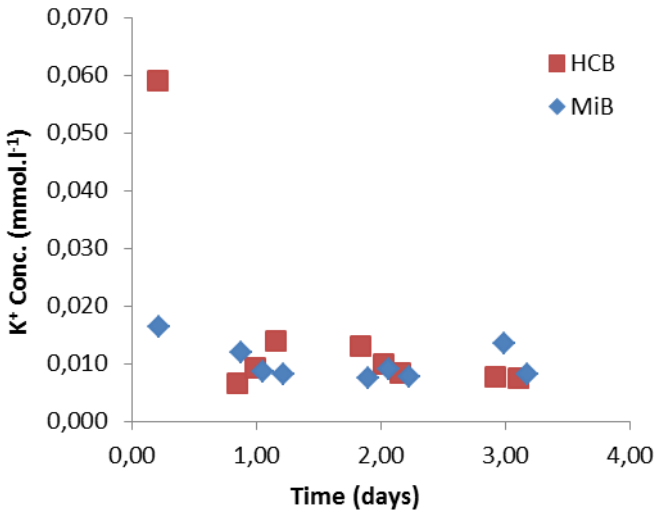

Figure 20. Concentration evolution for Potassium ion as function of time; steady state release rate is attained for both samples after the first day. The release rate of K^+ is steady for the micronized sample relative to HCB.

Release of Ca^{2+} and Mg^{2+} ions from HCB sample was uneven and reached their peak concentration 0.13mmol per liter at the second day. The pH measurement showed change in to alkaline and measurement form samples of second day read pH 8.4. In contrast release rate from sample MiB showed steady gradual decrease throughout the run.

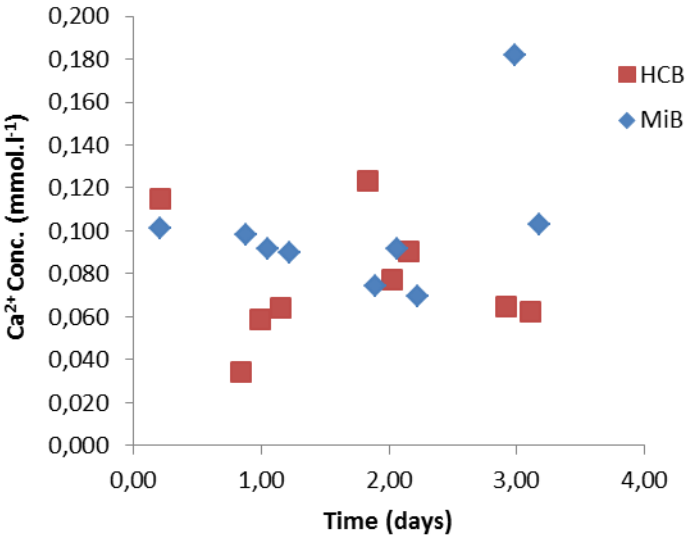

Figure 21. Change in concentration of Calcium ion as function of time; steady state release rate is attained at day two for both samples. MiB has relatively consistent release than HCB except to the increase in day three.

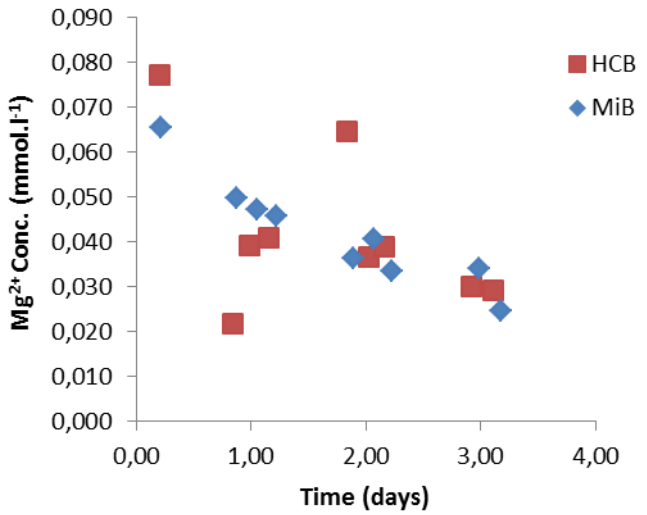

Figure 22. Change in concentration of Magnesium ion as function of time; Mg^{+2} releases from the MiB show steadily decreasing release rate with time relative to the HCB.

Silica has initial higher release that declines throughout the time log for both samples other than to the increase at slightly alkaline pH 7. 8.

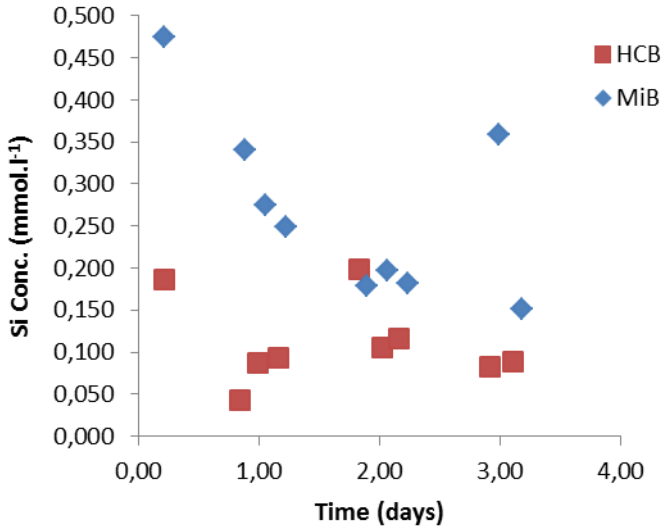

Figure 23. Silica released as function of time; for both samples steady state release rate attained after two days. The release rate is relatively consistent for the MiB in the first day.

The dissolution rate of basaltic glass at 80 ^{0}C and neutral pH shows initial decreasing phase and steady secondary phase in general for both samples. The relatively unclear separation between the phases and the inconsistent release of the ions in HCB may depict the effects of uneven grain size range and particle fractioning. The uneven particle distribution of sample HCB might exhibit the particle

distribution of natural weathering process and provide comparison with the pulverized sample to observe effect of reactive surface area on dissolution rate as function of time.

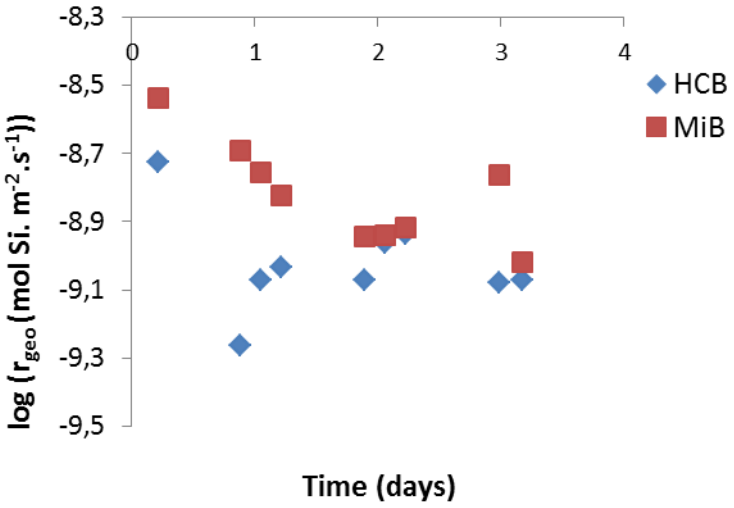

Figure 24. Logarithmic evolution of dissolution rate of basaltic glass based on the mole of Si during the flow through experiment performed at 80^0C and pH 7 as function of time for both hand crushed and micronized samples. The rate was calculated assuming the specific surface area remains constant.

The rate decreases initially and looks to attain steady state after the second day. The dissolution of the plant nutrients PO_4^{3-}, K^+ and in general the ions are higher for the micronized sample than the hand crushed. There is slight increase in release of K^+ from the HCB first to second day and this was the case for most of the cations. This could be due to pH favor as pH measurement on the samples taken on the first and second day showed 7.5 – 8.4. Generally all graphs have shown a decreasing release rate with time.

Steady state rate of dissolution of basaltic glass for the first experiment was calculated according to equation 3.2 at pH 7 and 80^0C (Table 4.3).

Table 4.3 rate of dissolution for both hand crushed and micronized samples in mol Si.$m^{-2}.s^{-1}$ calculated using equation 3.2

sample	mass(g)	Specific Surface area ($m^2.g^{-1}$)	Surface Area (m^2)	Flow rate ($g.s^{-1}$)	dCsi ($mol.g^{-1}$)	Rate (mol Si.$m^{-2}.s^{-1}$)
BDK	20	0,16	3,2	0,0316	8,55E-08	8,44E-10
BMI	10	0,52	5,2	0,0321	1,85E-07	1,15E-09

Table 4.3 shows that the dissolution rate of basaltic glass is higher for the micronized than the hand crushed. The difference in the rate of dissolution between hand crushed and micronized samples revealed that the higher surface area (depicted by the micronized sample) enhances the dissolution of basaltic glass.

Determining the phosphorus concentration associated to basaltic glass as fertilizer doesn't only define the amount of basalt required to obtain optimum P but can reduces eutrophication. Considering the basalt will completely dissolve, mass and percentage of phosphorus and other species element were calculated (Table 4.7) from the molecular formula given by (Stockmann et al., 2011) in chapter two.

Table 4.4 Elemental statistics of the basaltic glass used for this study. Mass and percentage of elements as well as molecular mass of the basaltic glass were computed.

Species	moles	Molar Mass (g/mol)	Mass Basalt (g)	in %
Si	1	28,086	28,086	22,57
Ti	0,025	47,867	1,196675	0,962
Al	0,365	26,982	9,84843	7,915
Fe	0,191	55,845	10,666395	8,572
Mn	0,003	54,94	0,16482	0,132
Mg	0,294	24,3	7,1442	5,742
Ca	0,263	40,1	10,5463	8,476
Na	0,081	22,99	1,86219	1,497
K	0,008	39,098	0,312784	0,251
p	0,004	30,97	0,12388	0,0996
O	3,405	15,999	54,476595	43,782
Molecular Mass			124,428269	

The approximated amount of the plant nutrients phosphorus and potassium according to above calculation is 0.1% and 0.25% respectively. Assuming constant specific surface area the moles of basaltic glass that could dissolve in a year from the initial 10g MiB was computed using;

$$n_b = n_0 - n_0 \exp^{-(k*s*m*t)} \quad \text{..... 4.1}$$

Accordingly, 0.073 moles of glass dissolve in a year, which is equivalent to 9.04g glass. Consequently, the amount of phosphorus and potassium that could be obtained from the 10g glass was $9.02*10^{-3}$g and 0.02g per year respectively.

Having all the above observations from the chemical analysis the tying question that should finally be addressed was, can basaltic glass be used as slow fertilizer? Modeling has been done in Matlab to emphasis the effect of change in specific surface area with time, temperature and pH in the dissolution of basaltic glass before answering this basic question. Moreover, the simulations will be compared to the experiment done at 80 ^{0}C and find out explanation for the decline in rate of release in the experimental results in relation to particle size distribution.

Analytical data such as particle size from LS-PSA, calculated specific rate constant and the specific surface area (cm^3) were used to simulate the dissolution rate of the hand crushed (BDK), micronized (BMI) and synthetic samples at different temperature and pH (Fig. 25 to 36). The simulation period was thirty days, 6 months and one year separately for each of the samples. The range of particle sizes for BDK and BMI are given in the method section (Fig.11&14) and temperature, rate constants as well as the pH used for the simulations are specified under each model.

4.2 Mat lab simulation results of HCB

The hand crushed sample was simulated for 30 days (model 1), six months (model 2) and one year (model 3) at temperatures 80^0C, 50^0C, 25^0C and pH of 8 as well as 4.

4.2.1 Model 1

Model one simulates dissolution of basaltic glass for 30 days at 80^0C and pH 8. The specific rate constant used in this simulation was $3.29*10^{-9}$ $mol.m^{-2}.s^{-1}$.

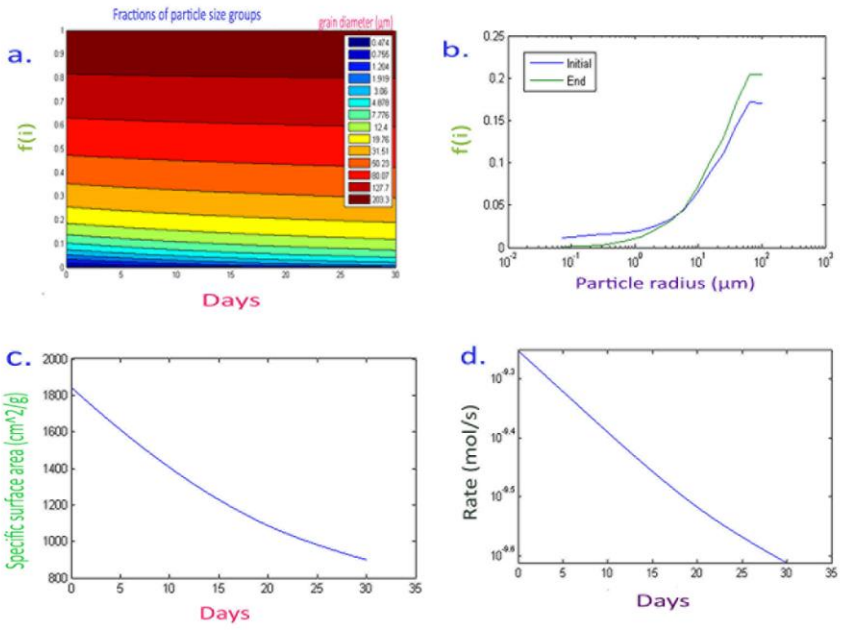

Figure 25. Illustrates simulation of basaltic glass dissolution rate for 30 days at 80^0C and pH 8; (a) fraction of individual particle size dissolving with time, (b) distribution of individuals fractions with respect to their particle radius as the reaction progress, (c) change in specific surface area ($cm^2 .g^{-1}$) with time and (d) rate of dissolution ($mol.s^{-1}$) as function of time.

The relative decrease in the fraction of individual particle sizes 0.47 - 4.878 µm shows all desolves at the end of the month (Fig. 25a). The shift in the distribution of the particle size (Fig. 25b) depicts the relative fraction of particles size 0.47 - 19.76 dissolved much as the reaction proogress. In addition, digestion of significant fractions of particle groups size 19.76 µm to 50.23µm increased initial specific surface area of reaction. Initially, the rate of reaction was $5.92*10^{-10}$ $mol.s^{-1}$. The coarser particles dominates the medium to the end (Fig. 25b) therefore, the release rate of the reaction declined to $3.62*10^{-10}$ $mol.s^{-1}$ in 25 days and decreases further with time (Fig. 25d).

Model 1 was also repeated by lowering the pH value. specific rate constant of $1.66*10^{-9}$ $mol.m^{-2}.s^{-1}$ was calculated for pH 4 providing the other parmeters remain the same.

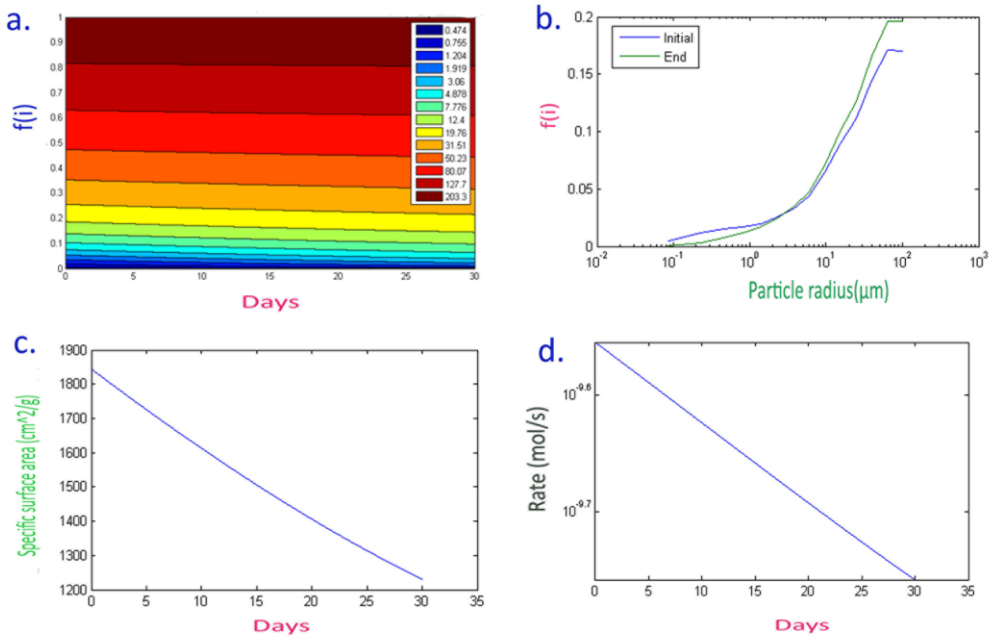

Figure 26. Demonstrates simulation of dissolution rate of basaltic glass for 30 days at 80^0C and pH 4; (a) fraction of individual particle size dissolving with time (b) distribution of individuals fractions with respect to their particle radius as the reaction progress, (c) change in specific surface area ($cm^2.g^{-1}$) with time and (d) rate of dissolution ($mol.s^{-1}$) as function of time

The initial rate in this model was $2.9*10^{-10}$ $mol.s^{-1}$, which is half of the initial rate of the alkaline pH, $5.9*10^{-10}$ $mol.s^{-1}$. The initial specific surface area, 1800 $cm^3.g^{-1}$ was reduced to $1300cm^3.g^{-1}$ and 900 $cm^2.g^{-1}$ at acidic and alkaline medium respectively. Hence, it infers for the same time period and temperature the dissolution rate was relatively high at pH 8 than pH 4. This might be due to the effect of temperature was high at alkaline pH.

4.2.2 Model 2

Specific rate constant of $5.27*10^{-10}$ $mol.m^{-2}.s^{-1}$, temprature 50^0C and pH 4 were considered to simulate the rate of disolution for Six months. Out put follows;

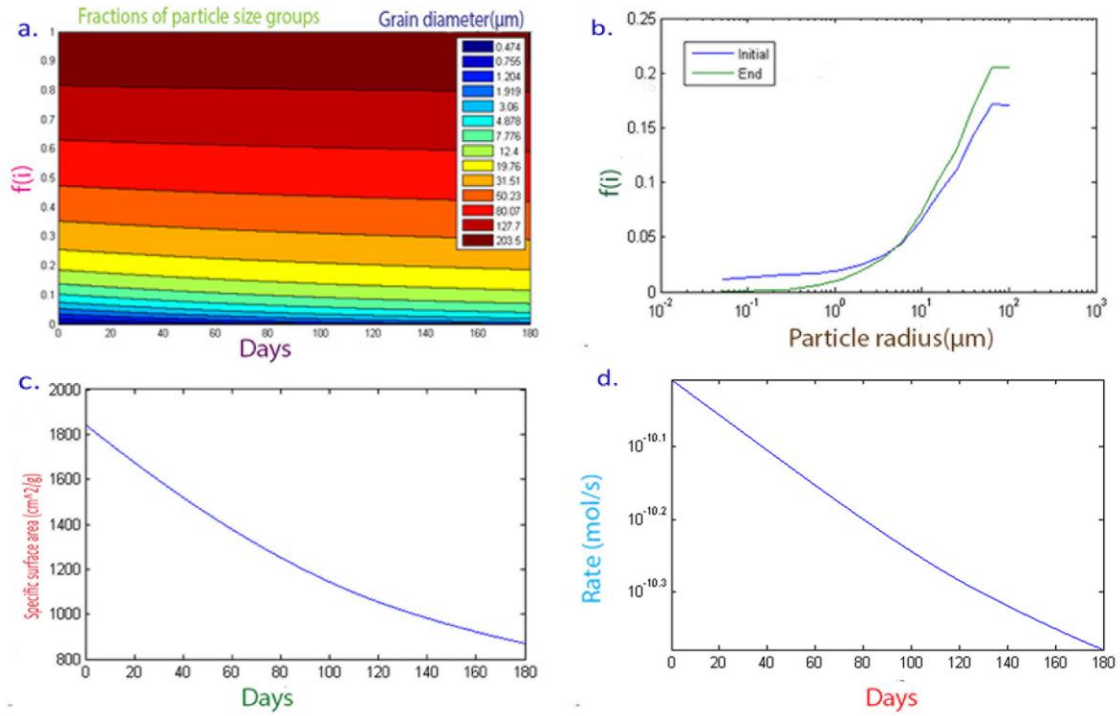

Figure 27. Basaltic glass dissolution rate simulation for 6 months at 50^0C and pH 4; (a) fraction of individual particle size as function of time, (b) fractions of particle size distribution as the reaction progress (c) change in specific surface area with time and (d) the rate of dissolution (mol.s^{-1}) as function of time

The initial rate is $1.06*10^{-10}$ mol.s^{-1}. At the beginning the reactive surface area about 1800cm^2.g^{-1} looks mainly to be contributed by the fine particles 0.474 to 7.776μm and reduces with time as these finer particle digested. The decline in surface area explains digestion of more fine particles, explained by the reduction in fractions of fine particles size to the end of the reaction (Fig. 27a). Moreover, the crossing of the green line in figure 27b also emphasis the dominancy of coarser particles at the end and the reduction of the rate by half in five months. At the 30^{th} day and pH 4 the rate in this model is about $8.4*10^{-11}$ mol.s^{-1}, which is five time less than the rate in model 1 at pH 4 and 30 days. This could mainly be due to the high temperature used in model 1.

4.2.3 Model 3

In this model the simulation time was extended to one year at temperature of 25^0C, pH 8 and specific rate constant, $2.61*10^{-10}$ mol.m^{-2}.s^{-1}.

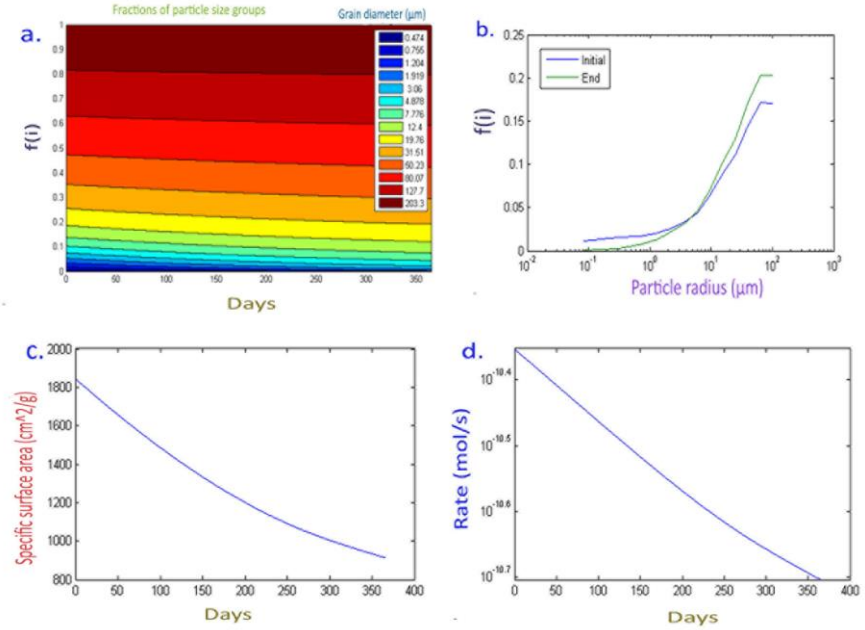

Figure 28. Illustrates simulation of Basaltic glass dissolution rate for a year at 25^0C and pH 8; (a) fraction of individual particle size dissolving with time, (b) distribution of individuals fractions with respect to their particle radius, (c) change in specific surface area (cm^2.g^{-1}) with time and (d) rate of dissolution (mol.s^{-1}) as function of time.

The digestion of the fraction of individual particle sizes 0.47 – 3.06µm took seven months (Fig. 28a). The particles size 4.878 – 19.76µm were digested to great extent in the given condition (Fig. 28a). Figure 28b indicates relative increase in coarser particles to the end of the reaction. Consequently, the specific surface area reduces by half in a year to 1000 cm^3 (Fig. 28c). As a result, the initial rate, $4.7*10^{-10}$ mol.s^{-1} declines by half, to $2.35*10^{-11}$ mol.s^{-1} at the end of the year.

4.3 Mat Lab Simulation Results of MiB

The micronized sample was also simulated similarly for thirty days (Simulation1), six months (Simulation 2) and one year (Simulation 3) at different temperaure and pH values.

4.3.1 simulation 1

The dissociation rate (mol/s) for the micronized basaltic glass was simulated for 30 days at 80^0C, pH 8 and specific rate constant of $3.29*10^{-9}$ mol.m^{-2}.s^{-1}.

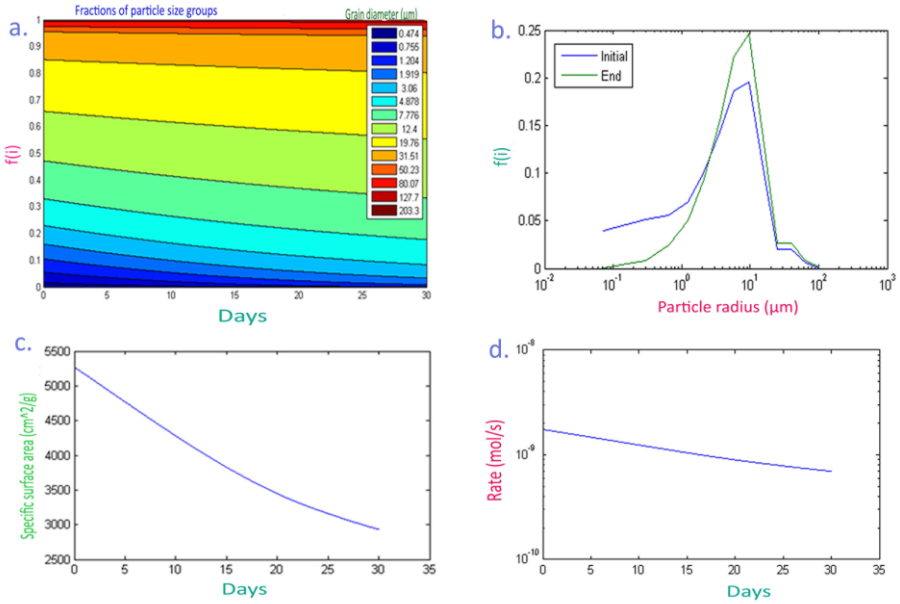

Figure 29. Illustrates simulation of basaltic glass dissolution rate for 30 days at 80^0C and pH of 8; (a) dissolving fractions of individual particle groups as function of time, (b distribution of fractions of particle with respect to their particle radius), (c) change in surface area of reaction with time (d) the rate of dissolution as function of time.

Particle sizes 0.474 -3.06 µm were completely dissolved and significant portion of particles radius of 4.878µm – 19.76µm dissolved in 30 days. Initially surface area was 5400cm^3 and provides initial rate $1.78*10^{-9}$ mol.s^{-1}. As the fractions of fine partilce size groups reduced to the end of the reaction the surface area decresed by 2500 cm^2.g^{-1} and hence the rate to $9.54*10^{-10}$ mol.s^{-1} . Provided the same temperature, pH and time the rate is high in this simulation due to high fractions of finer particle size groups relative to model 1 of HCB.

4.3.2 Simulation 2

Duration of 6 months, specific rate constant of $5.27*10^{-10}$ $mol.m^{-2}.s^{-1}$, temperature 50^0C and pH 4 are the conditions set for this simulation.

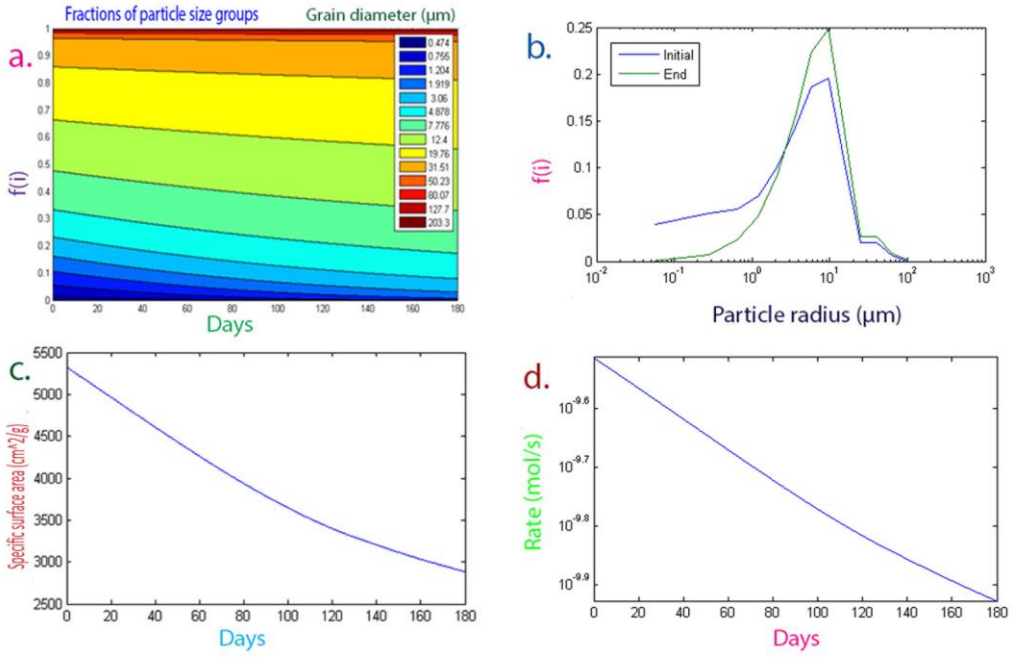

Figure 30. Basaltic glass dissolution rate simulation for 6 months at 50^0C and pH 4; (a) dissolving fractions of individual particle groups as function of time, (b distribution of fractions of particle with respect to their particle radius), (c) change in surface area of reaction with time (d) the rate of dissolution as function of time.

Complete dissolution of 0.474µm and 3.06µm lasted for four months in this model relative simulation 1. The initial surface area, $5400cm^3$ changes by 500 cm^3 in 20 days for this simulation and in 5 days difference for simulation 1. The initial rate, $2.85*10^{-10}$ $mol.s^{-1}$ declines to $1.58*10^{-10}$ mol.s-1 in 5 months. The rate of dissolution looks slow in this case.

4.3.3 Simulation 3

In this simulation specific rate constant, $2.61*10^{-10}$ $mol.m^{-2}.s^{-1}$ was used to model the dissolution rate of basaltic glass for one year at 25^0C and pH of 8.

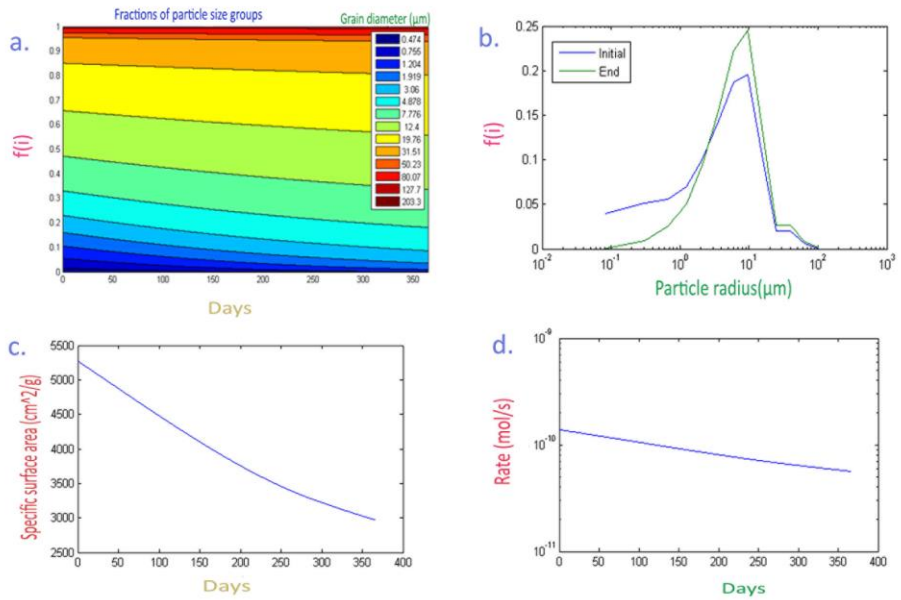

Figure 31. Basaltic glass dissolution rate simulation for one year at 25^0C and pH of 8; (a) dissolving fractions of individual particle groups as function of time, (b distribution of fractions of particle with respect to their particle radius), (c) change in surface area of reaction with time (d) the rate of dissolution as function of time.

In this model, fractions of particle sizes 1.204 µm to 1.919µm retained longer, less fractions of particle groups size 3.06µm to 19.76µm were dissolved in a year (Fig. 31a & c) relative to simulation 1 that has the same pH. Moreover, the specific surface area changes by 250cm^3 that is 10 times less than 2400cm^3 the change for simulation 1 in 30 days. Hence, the rate of dissolution is low as result of less dissolved surface are due to effect of low temperature. The removal of the fine particles reduced the surface area from 5400cm^3 to 3000cm^3 in a year. Subsequently, the dissolution rate looks steady at 7.8 * 10^{-11} mol.s^{-1}.

4.4 Mat lab simulation results of Synthetic Material (SB)

To estimate optimum possible particles size range that could digest fast and provide nutrients due to extended time, synthetic material of size ranges 0.390µm to 12.4µm were considered for one month and a year. The temperature, pH and rate constant were similar to model one of both hand crushed and micronized samples.

4.4.1 Model 1SB

Table 4.5. Grain size data and differential volume percent used in the simulation of the synthetic sample.

Grain diameter(µm)	0,39	0,575	0,843	1,504	2,019	4,106	5,878	7,776	12,4
Diif. Vol%	2,01	4,95	5,2	7,09	8,38	9,2	10,01	14,03	2,17

Simulation of this sample was done for 30 days at a temperature of 80^0C, pH of 8, calculated specific rate constant of $3.29*10^{-9}$ $mol.m^{-2}.s^{-1}$.

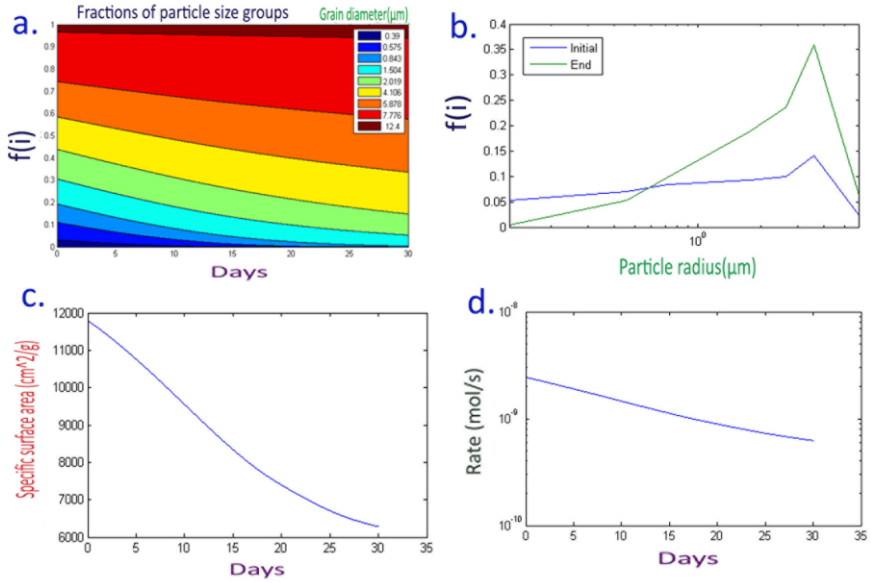

Figure 32. Simulation of dissolution rate of synthetic basaltic glass for 30 days at 80^0C and pH 8; (a) fraction of individual particle size with time, (b) fraction of individual grains variation fraction group number (c) Specific surface area of reaction versus time and (d) The rate of dissolution ($mol.s^{-1}$) of the basaltic glass with time.

Particle sizes 0.39µm to 0.843µm were completely dissolved in 20 days. The temperature, pH and rate constant were same with first models for MiB as well as HCB. The initial surface area, $12000cm^2.g^{-1}$ and rate, $3.95*10^{-9}mol.s^{-1}$, were double to that of simulation 1. This high surface area looks mainly provided by the first four fraction of particle size groups, 0.39µm to 1.5µm whereas half of it was provided by the first 7 fractions of particle size groups, 0.474µm to 7.776µm in simulation 1 and 3. Decline in the specific surface area to $6500cm^2.g^{-1}$ by the end of the month reduces the rate by half.

4.4.2 Model 2 SB

Same particles as model 1 SB were simulated for the one-year at 25^0C, pH 8 and specific rate constant $2.61*10^{-10}$ $mol.m^{-2}.s^{-1}$.

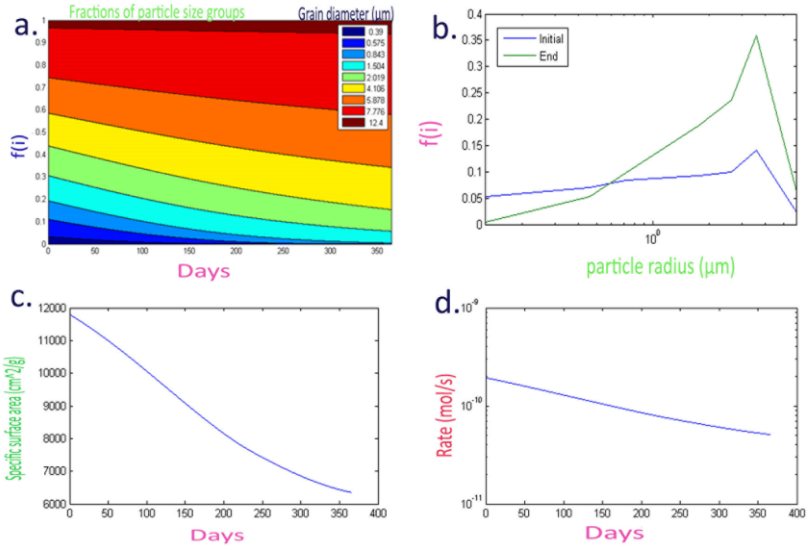

Figure 33. Simulation of dissolution rate of synthetic basaltic glass for one year at 25^0C and pH 8; (a) Dissolving fraction of individual particle size with time, (b) distribution of individual fractions of grains from initial to the end with respect to particle diameter (c) change in specific surface area of reaction as function of time and (d) The rate of dissolution (mol/s) of the basaltic glass with time.

The surface area reduced from 12000cm^3 to 6000 cm^3, particle size groups 0.39 µm – 1.504µm (Fig. 33a) were completely dissolved in a year. The fine particle sizes 0.39µm to 0.843µm dissolve completely in eight months and specific surface area changes by half in a year. Accordingly, the rate reduces from $3.13*10^{-10}$ mol.s^{-1} to $1.96*10^{-10}$ mol.s^{-1} in eight months and approaches zero as material continues to dissolve.

The flow through experiment and the Matlab simulations show the dissolution rates of the two samples were high at the beginning but decreases with time and change in grain size distribution. Initially the samples have higher concentration of fine grains that dissolve effectively at lower pH, but pH increases due to the buffering effect of the released cations. The release of cations Mg^{+2}, Ca^{+2}, K^+ followed by Silica was higher than the released concentration of the anion Fluorine and Sulfate ions. The relative consistency in the rate trend of MiB might be due to the similar range of grain size the medium it has.

Finally, the simulation has implicated that understanding the release rates from basaltic glass or any mineral fertilizers, knowledge of particle size distribution is crucial.

4.5 RESULT PART TWO

The concentration evolution of the plant nutrient (PO_4^{3-} & K^+), cations and Silica as a function of time are plotted in figure 34 and 35. Inference from the plots showed that there is reasonable high release of silica in the beginning of the reaction. Breaking of the silica network allowed phosphate and other ions to be released in to the solution as the concentration increases with time while silica is decreasing.

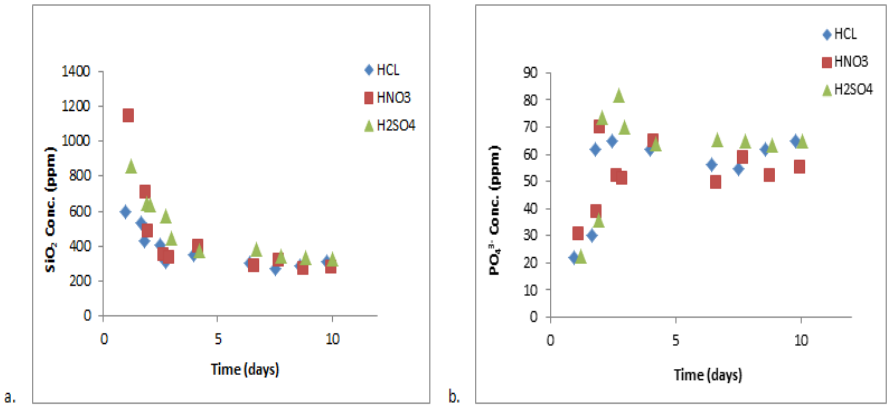

Figure 34. Change in concentration of Silica (a) and phosphate ion (b) as function of time after treating the basaltic glass with acids (given in the legend) at 90 ^{0}C and pH 0. The release rate of the phosphate ion and silica has negative correlation. PO_4^{3-} is better released relatively for the treatment with sulfuric acid.

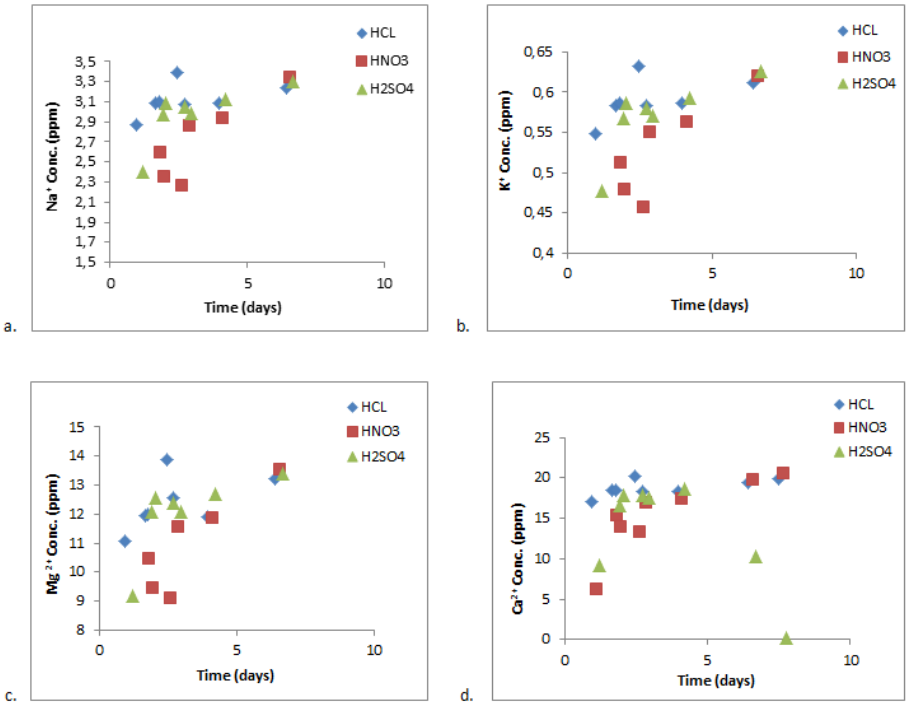

Figure 35. Change in concentration of cations Na^+ (a), K^+ (b), Mg^{2+} (c) and Ca^{2+} (d) with time after treating the basaltic glass with acids (shown in the legend) at 90 ^{0}C and pH 0. The release of the cations increases with time as a result of detaching the Si-bond after treating the glass with the acid. Sharp drop in concentration of Ca^{2+} was detected from the basalt treated with sulfuric acid (d) that will explain by SEM analysis below.

Both HCl and H_2SO_4 acid increase the digestion of basaltic glass relative to HNO_3 acid. Concentration of Calcium from the H_2SO_4 treated basalt glass showed a sharp drop after 19ppm in day eight (Fig. 35d). It could possibly be calcium was consumed into a solid phase. Release of Phosphate ion displays increasing first phase and steady second phase, while the cations increase throughout with decreasing release of silica for three of the samples. There is a negative correlation between release rate of silica and the ions at the provided condition.

There is 0.004 moles of phosphorus in the 124.4g of basalt given in table 4.4. Similar molecular formula basaltic glass of 5g contains $1.61*10^{-4}$ moles P or $4.99*10^{-3}$ g P. complete dissolution of 5g basaltic glass released all the $4.99 *10^{-6}$ kg P phosphorus.

SEM analysis of solid sample from the three reactors after moderate drying in the oven at 60 ^{0}C shows only silica phase. This shows then the complete release of the cations and anions into the bulk solution.

a.

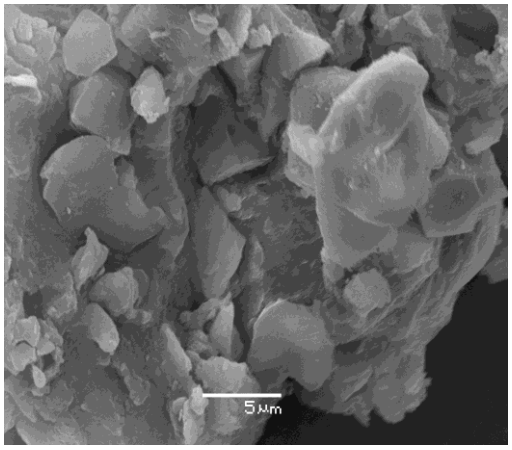

b.

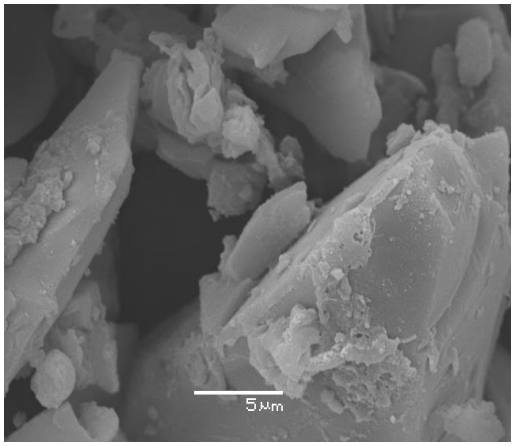

c.

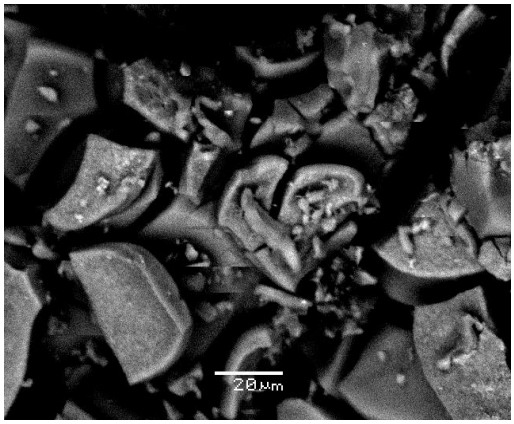

Figure 36. SEM analysis images of silica from dried solid samples of basaltic glass reacted with HCl (a) HNO_3 (b) and H_2SO_4 (c). Image c was not gold coated.

The Basalt treated with sulfuric acid though show formation of calcium sulphate mineral in the last days of the reaction. This could confirm the sharp decline in Ca^{2+}. The absence of other cations and anions in the solid sample could be a proof for their presence in the bulk solution samples.

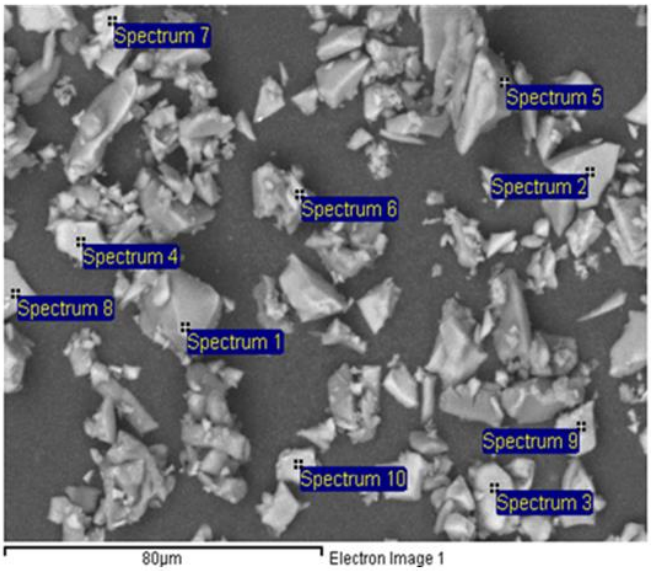

Spectrum	O	Si	Total
1	38,54	61,46	100
2	22,58	77,42	100
3	35,92	64,08	100
4	30	70	100
5	25,16	74,84	100
6	41,07	58,93	100
7	38,73	61,27	100
8	31,19	68,81	100
9	33,9	66,1	100
10	17,45	82,55	100
Mean	31,45	68,55	100
Std. deviation	7,73	7,73	
Max.	41,07	82,55	
Min.	17,45	58,93	

Figure 37. Illustrates random selection of grains for elemental analysis which Silicon and Oxygen are the constituents as the table of element statistics (%) at the right shows. This endorses the residual solid particles were pure silica and the other elements are in the liquid solutions.

SEM analysis shows calcium sulphate mineral was formed from the basaltic glass reacted with sulfuric acid. The sulfate ion was likely to be from the sulfuric acid used.

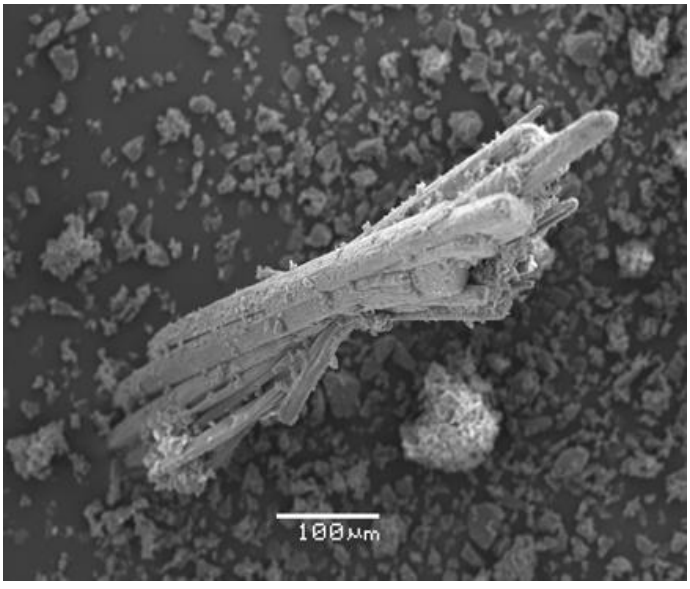

Figure 38. Calcium sulphate precipitated from the dissolved calcium and available sulfur (from sulfuric acid). Concentration of Ca^{2+} declined at the 8^{th} day due to formation of this mineral.

XRD analysis of the solid samples showed crystalline minerals of gypsum and pure silica at 90^0C and pH 0. Moreover, the SEM (Fig. 36) as well as XRD (Fig. 39) has showed the treatment of basaltic glass with these acids separated the silica from Aluminum, Iron, Other cations and anions.

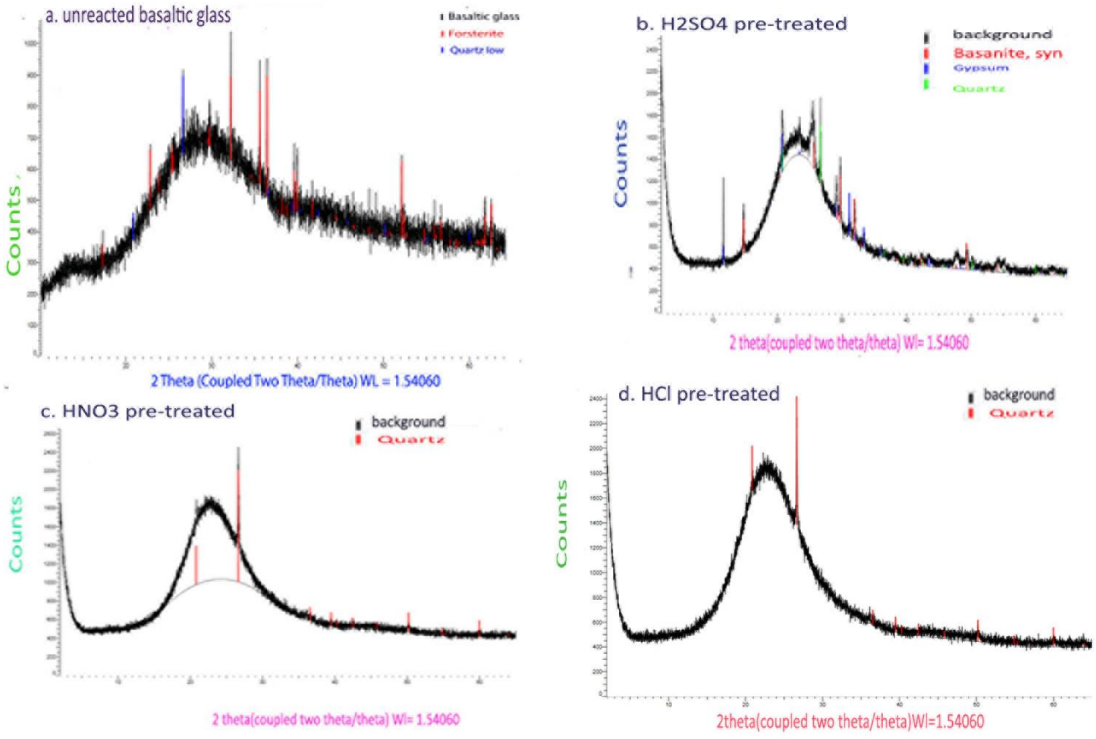

Figure 39. Illustrates contrast between XRD analysis spectrums of (a) unreacted basaltic glass (b) pre-treated with H_2SO_4 (c) pre-treated with HNO_3 and (d) pre-treated with HCl. The unreacted basaltic glass was described in Figure 7 that forsterite and quartz comprises 15% and the rest 85% was glass. The comparison reveals the formation of gypsum from the H_2SO_4 treated basaltic glass (Fig. 39b) and pure amorphous silica (described as background in b, c &d) after pre-treating the glass with the acids.

All the phosphorus in the basaltic glass was released to the aqueous solution and the possibility of precipitating as mineral fertilizer was modeled using Phreeqc. The simulation defines the possibility to precipitate the phosphate ion as Hydro- and Fluor-apatite. In addition, Brucite was also other mineral that has super saturated with the step wise increase moles of NaOH (Fig. 40).

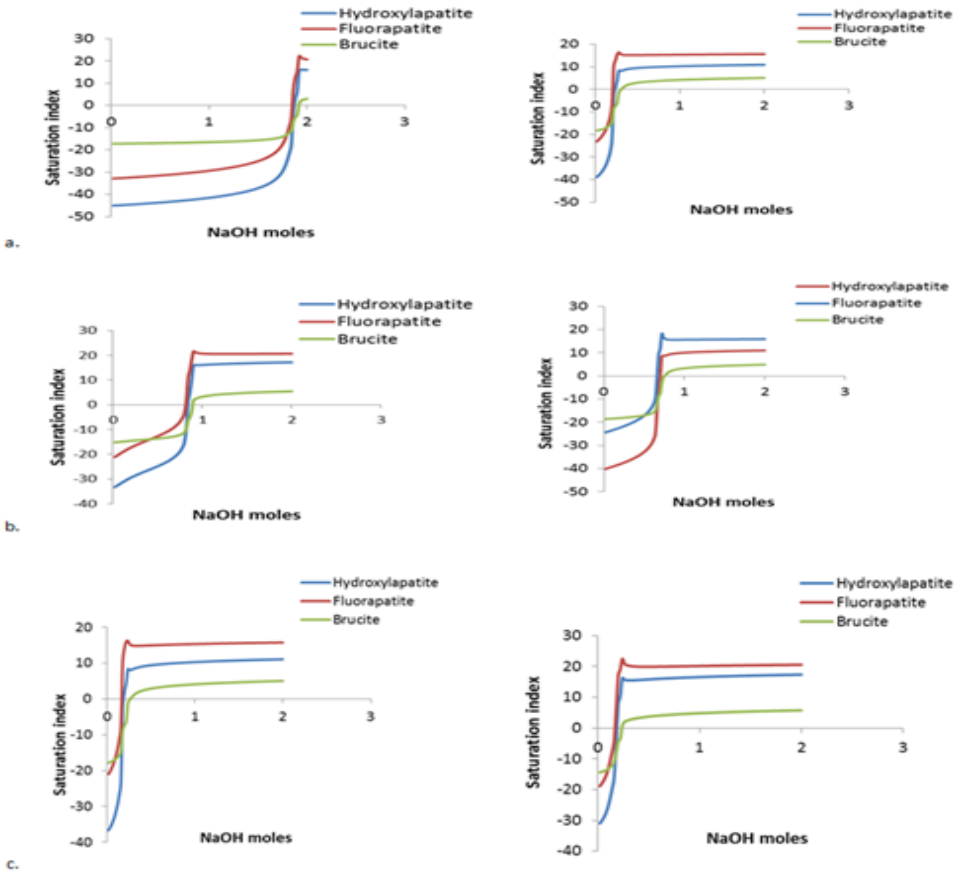

Figure 40. Saturation state of Hydroxylapatite, Fluorapatite and Brucite as a function of reaction progress between NaOH and pre-reacted aqueous solutions of HCl (a), H_2SO_4 (b) & HNO_3 (c) at 90 ^{0}C (left) and 25^{0}C (right).

The moles of NaOH required for super saturating the phosphate minerals (Fluorapatite and Hydroxylapatite) for the given concentration of the cations and orthophosphate ion varies among the three solutions and different temperature. This could be explained by the pH change as a function of moles of NaOH (Fig. 41). Moreover, the super saturation was attained fast at 25 ^{0}C with less moles of NaOH than at 90 ^{0}C, which can explain the nature of reaction of the ions with NaOH.

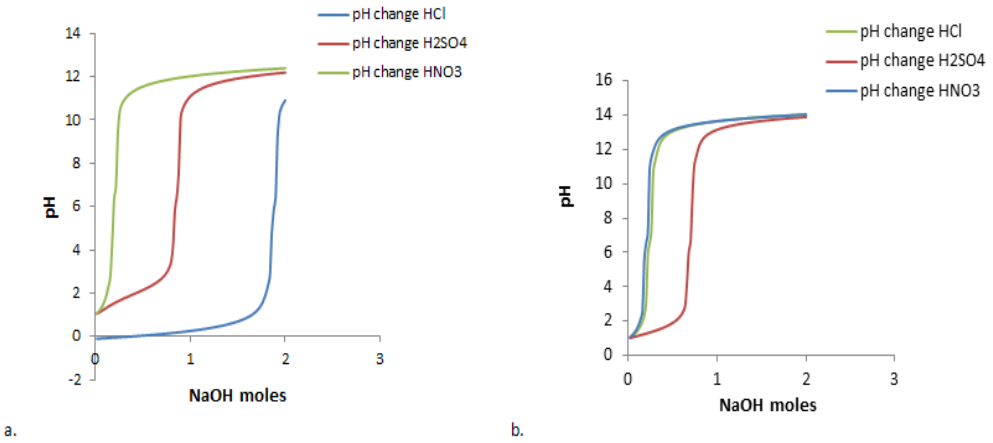

Figure 41. Change in pH as function of reaction progress between pre-reacted aqueous solution of HCl, H_2SO_4 and HNO_3 at 90^0C (a), 25^0C (b). The change in pH for the aqueous solution of HNO_3 and HCl was similar at 25 ^{0}C but different at 90 ^{0}C with increase in moles of NaOH.

The pH showed positive response to the increase in the NaOH and pH conditions that enable the super-saturating of the above mineral phases were reached.

5 DISCUSSIONS

5.1 DISCUSSION PART ONE

The pH dependency is known and since the dissolution leads to higher pH, rate increases in a soil with acidic pH and stabilizes with the pH buffering to neutral. Digestion of the monovalent and divalent cations from the surface of the basaltic glass at 80^0C and neutral condition depicts the high dissolution first phase. The pH measurement for the initial liquid samples lowers to 6.2. Steady state dissolution was attained after the second day of the reaction start and it looks the dissolution was independent of pH at the measured circum-neutral pH. Slight buffering effect was shown where the pH rise to 7.8 – 8.4 and dissolution of ions such as Ca, Na and Si responded to the change. Moreover, the release of mineral Ca, Mg and K in to the soil could alter the soil acidity. This was found to agree with (Heim et al., 2012) where they state the presence of these minerals increase the quality of the plant growth.

The flow through experiment and the Matlab simulations expresses the dissolution rates of the two samples decrease as function of time. The interpretation indicates the timely declining surface area mainly controlled the dissolution reaction and the longer the time of reaction enables utilization of the surface area of the large particles. Moreover, the simulation on the synthetic sample describes the dissolution is a relative selection of available particle sizes. Hence, there is no clear demarcation to determine optimum size range but it approves the finer the particles the higher will be the initial rates. Therefore, the early digestion of the finer particles modifies the size distribution, available surface area and kinetics of the reaction. Moreover, the effect of time was significant in this modeling as the one-year simulation for both samples has showed.

Relatively BMI has consistently decreasing rate compared to HCB, which could likely due to the larger range in grain size distribution of HCB**.** The relative high rate of micronized sample revealed the higher surface area enhanced the dissolution of basaltic glass. Similar observation has been also made by (Gislason and Oelkers, 2003)**.** The change in rate of dissolution modeled for three of the samples are negative as described by eq. (2.3).

Ranges of temperatures as well as pH were used for the Matlab modeling. The dissolution of basaltic glass shows low temperature dependency at pH 4 and high temperature dependency at pH 8. This is also in good agreement with the findings of (Helgeson et al., 1984) who noted pH independency at higher temperature and (Gudbrandsson et al., 2008) identify the high dependency of glass in temperature at alkaline pH.

The main objective was to quantify how much phosphorus (in the form of Orthophosphates) could be obtained from the dissolution of basaltic glass. Accordingly, complete dissolution of 10 g will release $3.2*10^{-4}$ moles P ($9.96*10^{-3}$ g) phosphorus as well as $6.43*10^{-4}$ moles (0.02g) K at 80^0C and pH 7.

Orthophosphates are the form of phosphate species that are edible by plants. The orthophosphate that can be formed from the dissolution of basaltic glass depends on the pH value. Hence, the term orthophosphate in this case stands for either HPO_4^{-2}, $H_2PO_4^-$ or PO_4^{-3}. The contrast between dissolution rate of basaltic glass as function of pH (Fig 16) with species abundance given in figure 6 depicts $H_2PO_4^-$ and HPO_4^{2-} are the dominant P species in the pH zones (pH 3 – 5 and 7 -10) respectively. Nevertheless, the dissolution of basalt glass at the circum-neutral pH zone was low though the proportionally occurrence of two species ($H_2PO_4^-$ and HPO_4^{2-}) could be important for plants.

For this study recommended concentration of plant nutrients for wheat described as 23-28kg P (Ross H., 2013) 28kg P and 140 kg K (Pathak et al., 2010) were considered as standard concentrations to determine the amount of basaltic glass. Amount of basaltic glass required per hectare per year was computed at 10 ^{0}C pH 4 using e.q 3.3 (details Appendix II), and were found 121,481.2 kg and 240,632.2 kg basalt per hectare per year for P and K respectively. Nitrate is the third plant nutrient specie but calculating the concentration of nitrate was ignored due to its negligible occurs in basaltic glass.

We see that the masses of basaltic glass required obtaining the standard amount of P and K are way too large. Moreover, for the hand crushed sample that has lower rate would be higher than these vales. Hence, two reasons could be described why direct use of basaltic glass is infeasible. First, the rate of dissolution of basaltic glass at neutral pH was too low.

Secondary, the actual pH in the agricultural fields is likely acidic that reduce the effect of low (relative to experiment temperature) actual temperature. In addition, the time considered was short to provide solid assessment of the possibility of development of secondary minerals at the surface of particles and sorption of phosphorus to developed clay mineral or hydroxides. Consequently, Basaltic glass can´t be used directly as source of fertilizer because of;

- The rate of P release is too low to deliver the required amount of P.
- The application of high mass of basaltic glass might cause accumulation of fluorine that lead to fluorine related environmental problems, and
- There might develop secondary minerals through time, which in turn could cause sorption effect and reduce the release of P.

Therefore, basaltic glass is not feasible to be applied directly as source of inorganic P fertilizer. But this result made us desperate to question the possibility of separating the nutrients and silica in the glass. Hence, pre-treating the glass with different acid types was conducted as second experiment to detach the plant nutrients and silica**.** Discussion follows.

5.2 DISCUSSION PART TWO

The plot of silica and phosphate indicates negative correlation (Fig. 37) because SiO_2 formed amorphous silica but phosphate was released completely. It can be also observed from Fig. 38 that the breaking of the Si-bonding has set the elements free as the cations concentration regularly increases with time. Hence, the more breakage of silica bonding would facilitate the release of cations and phosphate in to the solution. The decrease in the silica concentration with time looks due to SiO_2 formed amorphous silica whereas the other elements were released in to the solution (Fig. 36a-c). The concentration of the Ca^{2+} declined after the 8^{th} day for the treatment with sulfuric acid since the formation of gpsum was consuming the element (Fig. 39). This could reasonably explain the drop in the calcium concentration (figure 37d).

The EDS and XRD analysis of the solid sample reveals only pure silica structure and no Aluminum, implying Al could be released in to the bulk solution. This describes the complete release of phosphate and cations were dependent on the breakage silica structure. This goes in harmony with the explanation given by Guys and Scott, 1989 as well as Oelkers and Gislason, 2001. They showed that basaltic glass dissolution rate is proportional to the partially detached tetrahedral of silica. Separation of Silica and Aluminum reduces the possibility of formation of secondary clay minerals and the possible sorption of phosphorus. Therefore, this might then increase the amount of phosphorus released in to the bulk solution. The high initial silica release could be related to the fast dissolution property of basaltic glass in the strongly acidic medium and slowed down as the pH was buffered due to increased release of the cations (figures 34 & 35) as well as due to amorphous SiO_2 formation (Fig. 36). Similar observation was made in the work of (Gudbrandsson et al., 2011) where they noticed slow silica release from basaltic glass at higher temperature (75^0C) and alkaline pH. The treatment of basaltic glass with NaOH initially increased the release of silica but the main problem was the formation of Smectite.

The simulation using phreeqc showed that precipitation of the released phosphate ion likely in the form of Fluroapatite and Hydroapatite. The difference in the moles of NaOH consumed among the three solutions for the super saturated solutions depend on the reaction nature of the ions with respect to the pH change (Fig. 42). Moreover, at higher temperature more ions are released to the solution and

it is likely to form salts as well as ions that can act as weak acid. This might cause high moles of NaOH to be consumed to neutralize the pH as the reaction progresses (Fig. 41a-c left).

The solution being super saturated with Brucite, $Mg(OH)_2$, was also observed according to the geochemical modeling code phreeqc. This might increase the possibility of using basaltic glass as a fertilizer. High amount of basaltic glass is required as a source of phosphate fertilizer; hence considerable amount of Brucite might be formed. Brucite is identified as commercial flame-retardant and ore mineral for Mg due to its high Mg content. Moreover, advantageous of not releasing CO_2 in to the atmosphere (Simandl et al., 2007). We strongly believe that using basaltic glass in an environment friendly ways will boost its feasibility.

Super saturation of P in the forum of Fluorapatite could reduce the anthropogenic influence of soil environment in reference to the description given by (Loganthan eta al., 2008). They identify that the fluorine associated with $Ca_5(PO_4)_3F$ to be miner. This restrained the concern arose by EHS guidelines in 2007.

The complete release of phosphate was encouraging achievement and confirms possibility of basaltic glass as fertilizer source rock. But the cost of pretreatment may be high. Furthermore, the high amount of silica as a secondary product might be seen as environmental concern and cost exploiting in this case. Nevertheless, recently silica has attracted industrial demand. It is being used for many commercial purposes such as chips, optical fibers and telescope glasses. In addition, due to its mechanical resistance, high electrical strength and selectivity, amorphous silica was used as semiconductor in micro-electrons and chromatography (www.ks.uiuc.edu/Research/silica). The possibility to commercialize the amorphous silica and brucite could rather generate means of reimbursing the costs of processing the basaltic glass in to potential fertilizer. Moreover, this could also likely provide the fertilizer in cheap price and enable resource management.

6. CHAPTER SIX

6.1 CONCLUSION

Basaltic glass dissolution rate might be influenced by a number of factors such as pH change throughout the reaction, aqueous transport of species from the surface of the grains, temperature and the far from equilibrium conditions. The main objective of this study was to evaluate the feasibility of basaltic glass as potential source rock for phosphorus fertilizer. Experimental conditions were chosen to ensure that the rate is far from equilibrium and surface reaction controlled. The first experiment reveals the natural glass dissolution rate was so slow to deliver the required standard phosphorus concentration. As a result the basaltic glass doesn't look feasible to be used as source rock for phosphorus fertilizer directly may be due to one of the following reasons.

- The rate of P release was too low to supply the required amount of P by the plants.
- The application of high mass of basaltic glass might cause accumulation of fluorine that lead to fluorine related environmental problems.

Therefore, depending on this flow through result, it looks basaltic glass cannot be used directly as inorganic source of P fertilizer.

The second experimental result revealed the complete release of phosphate and makeover of pure amorphous silica. It showed the breaking of the Al-Si network setting free the essential nutrients in the glass for plant growth. This experimental result clearly showed that silica structure network in the basaltic glass influences the dissolution rate of basaltic glass and hence the release rate of P. This could be why release of P in the first experiment was low. Provided the basaltic glass is pretreated it could furnish the whole amount of P and could possibly be precipitated in the form of Hydro-and/or Fluor-apatite to be used as fertilizer. Hence, basaltic glass might be feasible inorganic source rock for fertilizer after treated with acids. But the cost of pretreatment might be high. If the byproducts such as amorphous silica and brucite have the possibility to be commercialized, they could probably create an alternative solution to cover the costs associated to the processing of pretreatment of basaltic glass. This could perhaps provide the fertilizer in cheap price and enable feasibility of basaltic glass as source for fertilizer.

As a possible alternative, mining the resource for the purpose of silica production and separating the plant nutrients for fertilization could also be a way to use the resource as source of P fertilizer. In this case the other released elements, such as Si and Mg, are foreseen to be the main product of the acid

treatment with possible commercial purposes and the plant nutrients as by product would be used for fertilizer.

6.2 RECOMMENDATION

The experiments were conducted for a very short period of time and relatively at higher temperatures compared to the soil environment. Therefore we recommend longer time experiments at a soil temperature condition because this could provide essential data on the natural dissolution of the basaltic glass as well as about the possibility of formation of secondary mineral phases from the direct use and acid treatment.

Moreover, further experimental study on the possibility of crystallizing the silica would be done to explore the multipurpose utilization of basaltic glass. Last but not least, studying the basaltic glass dissolution rate in the presence of the actual soil environment could also be advisable as soil types may affect the dissolution rate of basaltic glass and hence affect the potential of basaltic glass a source fertilizer.

REFERENCES

Aulakh, M. S., Kabba, B. S., Baddesha, H. S., Bahl, G. S., and Gill, M. P. S., 2003, Crop yields and phosphorus fertilizer transformations after 25 years of applications to a subtropical soil under groundnut-based cropping systems: Field Crops Research, v. 83, no. 3, p. 283-296.

Berger, G., Schott, J., and Guy, C., 1988, Behavior of Li, Rb and Cs during basalt glass and olivine dissolution and chlorite, smectite and zeolite precipitation from seawater: Experimental investigations and modelization between 50° and 300°C: Chemical Geology, v. 71, no. 4, p. 297-312.

Berger, G., Schott, J., and Loubet, M., 1987, Fundamental processes controlling the first stage of alteration of a basalt glass by seawater: an experimental study between 200 and 320 C: Earth and Planetary Science Letters, v. 84, no. 4, p. 431-445.

Brunet, F., and Chazot, G., 2001, Partitioning of phosphorus between olivine, clinopyroxene and silicate glass in a spinel lherzolite xenolith from Yemen: Chemical Geology, v. 176, no. 1–4, p. 51-72.

Chen, G. C., He, Z. L., Stoffella, P. J., Yang, X. E., Yu, S., and Calvert, D., 2006, Use of dolomite phosphate rock (DPR) fertilizers to reduce phosphorus leaching from sandy soil: Environmental Pollution, v. 139, no. 1, p. 176-182.

Cooper, J., Lombardi, R., Boardman, D., and Carliell-Marquet, C., 2011, The future distribution and production of global phosphate rock reserves: Resources, Conservation and Recycling, v. 57, no. 0, p. 78-86.

Cordell, D., Drangert, J.-O., and White, S., 2009, The story of phosphorus: Global food security and food for thought: Global Environmental Change, v. 19, no. 2, p. 292-305.

Dawson, C. J., and Hilton, J., 2011, Fertiliser availability in a resource-limited world: Production and recycling of nitrogen and phosphorus: Food Policy, v. 36, Supplement 1, no. 0, p. S14-S22.

Devau, N., Cadre, E. L., Hinsinger, P., Jaillard, B., and Gérard, F., 2009, Soil pH controls the environmental availability of phosphorus: Experimental and mechanistic modelling approaches: Applied Geochemistry, v. 24, no. 11, p. 2163-2174.

EHS, 2007, Environmental, Health and Safety Guidelines for Phosphate Fertilizer Manufacturing: IFC, p. 20.

Gilbert, N., 2009, The disappearing nature: nature v. 461, p. 3.

Gislason, S. R., and Oelkers, E. H., 2003, Mechanism, rates, and consequences of basaltic glass dissolution: II. An experimental study of the dissolution rates of basaltic glass as a function of pH and temperature: Geochimica et Cosmochimica Acta, v. 67, no. 20, p. 3817-3832.

Gudbrandsson, S., Wolff-Boenisch, D., Gislason, S., and Oelkers, E., 2008, Dissolution rates of crystalline basalt at pH 4 and 10 and 25–75 C: Mineralogical Magazine, v. 72, no. 1, p. 155-158.

Gudbrandsson, S., Wolff-Boenisch, D., Gislason, S. R., and Oelkers, E. H., 2011, An experimental study of crystalline basalt dissolution from 2 ⩽ pH ⩽ 11 and temperatures from 5 to 75 °C: Geochimica et Cosmochimica Acta, v. 75, no. 19, p. 5496-5509.

Gustafsson, J. P., Mwamila, L. B., and Kergoat, K., 2012, The pH dependence of phosphate sorption and desorption in Swedish agricultural soils: Geoderma, v. 189, p. 304-311.

Guy, C., and Schott, J., 1989, Multisite surface reaction versus transport control during the hydrolysis of a complex oxide: Chemical Geology, v. 78, no. 3–4, p. 181-204.

Hanrahan, G., Salmassi, T. M., Khachikian, C. S., and Foster, K. L., 2005, Reduced inorganic phosphorus in the natural environment: significance, speciation and determination: Talanta, v. 66, no. 2, p. 435-444.

Harley, A., and Gilkes, R., 2000, Factors influencing the release of plant nutrient elements from silicate rock powders: a geochemical overview: Nutrient Cycling in Agroecosystems, v. 56, no. 1, p. 11-36.

Heffer, P., and Prud'homme, M., 2012, Fertilizer outlook in 2012-2016: International Fertilizer Association (IFA), v. A/12/69, p. 7.

Heffer, P., and Prud'homme, M., Fertilizer Outlook 2010-2014, *in* Proceedings 78th IFA Annual Conference, Paris2010.

Heim, M., Hillersøy, M. H., Bleken, M. A., Gautneb, H., and Gjengedal, E. L., 2012, APATITE–BIOTITE–CARBONATITE (STJERNØY, N-NORWAY) – POTENTIAL AND OBSTACLES REGARDING A MULTINUTRIENT ROCK-FERTILIZER: International Congress for Applied Mineralogy (ICAM), p. 8.

Helgeson, H. C., Murphy, W. M., and Aagaard, P., 1984, Thermodynamic and kinetic constraints on reaction rates among minerals and aqueous solutions. II. Rate constants, effective surface area, and the hydrolysis of feldspar: Geochimica et Cosmochimica Acta, v. 48, no. 12, p. 2405-2432.

Hendrix, J. L., 2012, Sustainable Agricultural Practices Impact on Phosphate rock production: Procedia Engineering, v. 46, no. 0, p. 54-61.

Loganathan, P., and Hedley, M. J., 1997, Downward movement of cadmium and phosphorus from phosphatic fertilisers in a pasture soil in New Zealand: Environmental Pollution, v. 95, no. 3, p. 319-324.

Loganathan, P., Hedley, M. J., and Grace, N. D., 2008, Pasture soils contaminated with fertilizer-derived cadmium and fluorine: livestock effects, Reviews of environmental contamination and toxicology, Springer, p. 29-66.

Loganathan, P., Hedley, M. J., Wallace, G. C., and Roberts, A. H. C., 2001, Fluoride accumulation in pasture forages and soils following long-term applications of phosphorus fertilisers: Environmental Pollution, v. 115, no. 2, p. 275-282.

Manoharan, V., Loganathan, P., Tillman, R. W., and Parfitt, R. L., 2007, Interactive effects of soil acidity and fluoride on soil solution aluminium chemistry and barley (Hordeum vulgare L.) root growth: Environmental Pollution, v. 145, no. 3, p. 778-786.

McDowell, R. W., Monaghan, R. M., and Carey, P. L., 2003, Potential phosphorus losses in overland flow from pastoral soils receiving long‐term applications of either superphosphate or reactive phosphate rock: New Zealand Journal of Agricultural Research, v. 46, no. 4, p. 329-337.

Mezghani, I., Elloumi, N., Abdallah, F. B., Chaieb, M., and Boukhris, M., 2005, Fluoride accumulation by vegetation in the vicinity of a phosphate fertilizer plant in Tunisia: Fluoride, v. 38, no. 1, p. 18-24.

Morgan, N. A., and Spera, F. J., 2001, Glass transition, structural relaxation, and theories of viscosity: a molecular dynamics study of amorphous CaAl< sub> 2</sub> Si< sub> 2</sub> O< sub> 8</sub>: Geochimica et Cosmochimica Acta, v. 65, no. 21, p. 4019-4041.

Nesbitt, H., and Young, G., 1984, Prediction of some weathering trends of plutonic and volcanic rocks based on thermodynamic and kinetic considerations: Geochimica et Cosmochimica Acta, v. 48, no. 7, p. 1523-1534.

Oelkers, E. H., and Gislason, S. R., 2001, The mechanism, rates and consequences of basaltic glass dissolution: I. An experimental study of the dissolution rates of basaltic glass as a function of aqueous Al, Si and oxalic acid concentration at 25°C and pH = 3 and 11: Geochimica et Cosmochimica Acta, v. 65, no. 21, p. 3671-3681.

Pathak, H., Mohanty, S., Jain, N., and Bhatia, A., 2010, Nitrogen, phosphorus, and potassium budgets in Indian agriculture: Nutrient Cycling in Agroecosystems, v. 86, no. 3, p. 287-299.

Pickering, H. W., Menzies, N. W., and Hunter, M. N., 2002, Zeolite/rock phosphate—a novel slow release phosphorus fertiliser for potted plant production: Scientia Horticulturae, v. 94, no. 3–4, p. 333-343.

Ross H., M., Allan Middleton, 2013, Phosphorus Fertilizer Application in Crop Production: Alberta Agriculture and Rural Development, Research and Innovation Division, Agriculture Centre, Lethbridge, p. 1-12.

Rowe Jr, G. L., and Brantley, S. L., 1993, Estimation of the dissolution rates of andesitic glass, plagioclase and pyroxene in a flank aquifer of Poas Volcano, Costa Rica: Chemical Geology, v. 105, no. 1, p. 71-87.

Ryan, J., Ibrikci, H., Delgado, A., Torrent, J., Sommer, R., and Rashid, A., 2012, Chapter three - Significance of Phosphorus for Agriculture and the Environment in the West Asia and North Africa Region, *in* Donald, L. S., ed., Advances in Agronomy, Volume Volume 114, Academic Press, p. 91-153.

Sheldon, R. P., 1982, Phosphate Rock: SCIENTIFIC AMERICAN, v. 246, p. 7.

Simandl, G. J., Paradis, S., and Irvine, M., 2007, Brucite-industrial mineral with a future: Geoscience Canada, v. 34, no. 2.

Smith, I. E. M., Ward, G. K., and Ambrose, W. R., 1978, Geographic Distribution and the Characterization of Volcanic Glasses in Oceania: Oceania Publications, University of Sydney collaborating with JSTOR, v. 12, p. 30.

Smith, J. V., 1981, Halogen and phophorus storage in the earth: Nature, v. 289, p. 762-764.

Stockmann, G. J., Wolff-Boenisch, D., Gislason, S. R., and Oelkers, E. H., 2011, Do carbonate precipitates affect dissolution kinetics? 1: Basaltic glass: Chemical Geology, v. 284, no. 3–4, p. 306-316.

Suh, S., and Yee, S., 2011, Phosphorus use-efficiency of agriculture and food system in the US: Chemosphere, v. 84, no. 6, p. 806-813.

Takahashi, S., and Anwar, M. R., 2007, Wheat grain yield, phosphorus uptake and soil phosphorus fraction after 23 years of annual fertilizer application to an Andosol: Field Crops Research, v. 101, no. 2, p. 160-171.

White, A. F., and Brantley, S. L., 2003, The effect of time on the weathering of silicate minerals: why do weathering rates differ in the laboratory and field?: Chemical Geology, v. 202, no. 3–4, p. 479-506.

Wolff-Boenisch, D., Gislason, S. R., and Oelkers, E. H., 2004a, The effect of fluoride on the dissolution rates of natural glasses at pH 4 and 25°C: Geochimica et Cosmochimica Acta, v. 68, no. 22, p. 4571-4582.

Wolff-Boenisch, D., Gislason, S. R., Oelkers, E. H., and Putnis, C. V., 2004b, The dissolution rates of natural glasses as a function of their composition at pH 4 and 10.6, and temperatures from 25 to 74°C: Geochimica et Cosmochimica Acta, v. 68, no. 23, p. 4843-4858.

Yang, Y., He, Z., Yang, X., Fan, J., Stoffella, P., and Brittain, C., 2012, Dolomite Phosphate Rock–Based Slow-Release Fertilizer for Agriculture and Landscapes: Communications in Soil Science and Plant Analysis, v. 43, no. 9, p. 1344-1362.

http://www.geoforskning.no/index.php?option=com_content&view=article&id=495:mineralavfall-kan-redusere-klimagassutslipp&catid=23:co2&Itemid=218 (accessed 13 august, 2013)

http://www.fertilizer.org/ifa/HomePage/Statistics/Production-and-trade (accessed 01 November, 2013)

http://www.ks.uiuc.edu/Research/silica (accessed on 03 january, 2014)

APPENDIX I: Results and procedures used for the flow through experiment

A. Sampling chart and particle size measurement

Table 1 data chart for the mixed flow through performed at 80 ^{0}C and neutral pH

		Day One						
Reservoir	**Sample name**	**Bottle Wt. (g)**	**Total Wt. (g)**	**Solution Wt. (g)**	**Sampling start time**	**Total time(min)**	**Rate (g/min)**	**Date**
R4	BDK	10	29,5	19,5	17:00	10	1,95	26-03-13
R5	BMI	10,1	28,8	18,7	17:02	10	1,87	26-03-13
		Day Two						
R4	BDK	10	29,5	19,5	09:16	10	1,95	27-03-13
R5	BMI	9,9	28,2	18,3	10:16	10	1,83	27-03-13
R4	BDK	10,1	28,8	18,7	11:16	10	1,87	27-03-13
R5	BMI	10	29,6	19,6	12:16	10	1,96	27-03-13
R4	BDK	9,9	28,9	19	17:07	10	1,9	27-03-13
R5	BMI	10	28,5	18,5	17:09	10	1,85	27-03-13
		Day Three						
R4	BDK	10	28,6	18,6	09:29	10	1,86	28- 03-13
R5	BMI	10	29,6	19,6	09:26	10	1,96	28- 03-13
R4	BDK	10	29,9	19,9	13:35	10	1,99	28- 03-13
R5	BMI	10	27,8	17,8	13:37	10	1,78	28- 03-13
R4	BDK	10	29,1	19,1	17:05	10	1,91	28- 03-13
R5	BMI	10	30,4	20,4	17:07	10	2,04	28- 03-13

		Day Four						
R4	BDK	10	29,5	19,5	09:23	10	1,95	29-03-13
R5	BMI	10,1	27,3	17,2	09:20	10	1,72	29-03-13
R4	BDK	10	28,4	18,4	13:15	10	1,84	29-03-13
R5	BMI	10	29,5	19,5	13:17	10	1,95	29-03-13

B. CALCULATING THE RATE TO ESTIMATE THE FLOW RATE FOR THE MIXED FLOW EXPERIMENT

$r = K_1^T * a_H^{+n_1} + K_2^T + K_3^T * a_H^{+n_3}$ …….. 1

r is rate (mol.cm^{-2}.s^{-1}), k rate constant (mol.cm^{-2}.s^{-1}) , a_{H+} activity of hydrogen ion and n is slope of the rate graph

$log r = \log(K_1^T * a_H^{+n_1} + K_2^T + K_3^T * a_H^{+\ n_3})$……...2

The value of K_i^T (i=1, 2 & 3) can be calculated according to Arrhenius equation. Hence;

$K_1^T = k^0 * e^{-\frac{E_a}{R}\left(\frac{1}{\Delta T}\right)}$ ……..3

k^0 is specific rate constant at 25^{0}C. From eq. 3 K_1^T, K_2^T and K_3^T are equal to their respective k^0. Hence, at 25^{0}C eq. 2 would be;

$log r = \log(k_1^0 * a_{H_+}^{n_1} + k_2^0 + k_3^0 * a_H^{+\ n_3})$…….. 4

To calculate k_1^0 at pH= 0 we consider $\log k_2^0 + \log(k_3^0 * a_H^{+\ n_3})$ is zero. Therefore;

$log r = \log k_1^0$ ……. 5

The same procedure was done to calculate k_2^0 and k_3^0. After this K_1^T , K_2^T and K_3^T are calculated based on equation 3.

n_1, n_2 and n_3 are the slopes of the graph drown at 25^{0}C for the log r and pH. They are calculated according to general formula $n = \frac{\Delta y}{\Delta x}$.

$n_1 = \frac{\Delta \log r}{\Delta \mathrm{pH}}$…… 6

n_2 and n_3 were calculated likewise and Calculation results are given in Table 3 -8 with respect to their temperature and sample name.

Table 3. Calculated rate of dissolution (mol/cm^2/s) at 25^{0}C for sample HCB based on equation 3.2

pH	$K_1T'*a_{H+}^n$	$K_2T*a_{H+}^n$	$K_3T*a_{H+}^n$	r (mol/cm^2/s)	Log r	s(m^2/g)
0	1,00E-17	1,00E-15	5,01E-10	5,01E-10	-9,3	0,16
1	3,55E-17	1,00E-15	3,98E-11	3,98E-11	-10,4	0,16
2	1,26E-16	1,00E-15	3,16E-12	3,16E-12	-11,5	0,16
3	4,47E-16	1,00E-15	2,51E-13	2,53E-13	-12,6	0,16
4	1,58E-15	1,00E-15	2,00E-14	2,25E-14	-13,65	0,16
5	5,62E-15	1,00E-15	1,58E-15	8,21E-15	-14,09	0,16
6	2,00E-14	1,00E-15	1,26E-16	2,11E-14	-13,68	0,16
7	7,08E-14	1,00E-15	1,00E-17	7,18E-14	-13,14	0,16
8	2,61E-13	1,00E-15	7,94E-19	2,62E-13	-12,6	0,16
9	8,91E-13	1,00E-15	6,31E-20	8,92E-13	-12,05	0,16
10	3,16E-12	1,00E-15	5,01E-21	3,16E-12	-11,5	0,16

Table 4. calculated rate of dissolution (mol/cm^2/s) at 25^{0}C for sample MiB based on equation 3.2

pH	$K_1T'*a_{H+}^n$	$K_2T*a_{H+}^n$	$K_3T*a_{H+}^n$	r (mol/cm^2/s)	Log r	s(m^2/g)
0	1,00E-17	1,00E-15	5,01E-10	5,01E-10	-9,3	0,51
1	3,55E-17	1,00E-15	3,98E-11	3,98E-11	-10	0,51
2	1,26E-16	1,00E-15	3,16E-12	3,16E-12	-12	0,51
3	4,47E-16	1,00E-15	2,51E-13	2,53E-13	-13	0,51
4	1,58E-15	1,00E-15	2,00E-14	2,25E-14	-14	0,51
5	5,62E-15	1,00E-15	1,58E-15	8,21E-15	-14	0,51
6	2,00E-14	1,00E-15	1,26E-16	2,11E-14	-14	0,51
7	7,08E-14	1,00E-15	1,00E-17	7,18E-14	-13	0,51
8	2,51E-13	1,00E-15	7,94E-19	2,62E-13	-13	0,51
9	8,91E-13	1,00E-15	6,31E-20	8,92E-13	-12	0,51
10	3,16E-12	1,00E-15	5,01E-21	3,16E-12	-12	0,51

Table 5: rate of reaction (mol/s) calculated at 50^{0}C for sample HCB based on equation 3.2

pH	$K_1T'*a_{H+}^n$	$K_2T*a_{H+}^n$	$K_3T*a_{H+}^n$	r (mol/cm^2/s)	Log r	s(m^2/g)
0	1,39E-09	2,78E-15	3,50E-18	1,39E-09	-8,86	0,16
1	1,10E-10	2,78E-15	1,24E-17	1,10E-10	-9,96	0,16
2	8,77E-12	2,78E-15	4,40E-17	8,77E-12	-11,06	0,16
3	6,96E-13	2,78E-15	1,56E-16	6,99E-13	-12,16	0,16
4	5,54E-14	2,78E-15	5,54E-16	5,87E-14	-13,23	0,16
5	4,40E-15	2,78E-15	1,97E-15	9,14E-15	-14,04	0,16
6	3,49E-16	2,78E-15	6,98E-15	1,01E-14	-14,00	0,16
7	2,77E-17	2,78E-15	2,47E-14	2,76E-14	-13,56	0,16
8	2,20E-18	2,78E-15	4,99E-14	5,27E-14	-13,28	0,16
9	1,75E-19	2,78E-15	3,12E-13	3,15E-13	-12,50	0,16
10	1,39E-20	2,78E-15	1,11E-12	1,11E-12	-11,95	0,16

Table 6. Rate of reaction (mol/s) calculated at 50^0C for sample MiB based on eq. (2.1)

pH	$K_1T'*a_{H+}^n$	$K_2T*a_{H+}^n$	$K_3T*a_{H+}^n$	r (mol/cm^2/s)	Log r	s(m^2/g)
0	1,39E-09	2,78E-15	3,50E-18	1,39E-09	-8,86	0,16
1	1,10E-10	2,78E-15	1,24E-17	1,10E-10	-9,96	0,16
2	8,77E-12	2,78E-15	4,40E-17	8,77E-12	-11,06	0,16
3	6,96E-13	2,78E-15	1,56E-16	6,99E-13	-12,16	0,16
4	5,54E-14	2,78E-15	5,54E-16	5,87E-14	-13,23	0,16
5	4,40E-15	2,78E-15	1,97E-15	9,14E-15	-14,04	0,16
6	3,49E-16	2,78E-15	6,98E-15	1,01E-14	-14,00	0,16
7	2,77E-17	2,78E-15	2,47E-14	2,76E-14	-13,56	0,16
8	2,20E-18	2,78E-15	4,99E-14	5,27E-14	-13,28	0,16
9	1,75E-19	2,78E-15	3,12E-13	3,15E-13	-12,50	0,16
10	1,39E-20	2,78E-15	1,11E-12	1,11E-12	-11,95	0,16

Table 7: rate of reaction (mol/s) calculated at 75^0C for sample HCB based on eq. (2.1)

pH	$K_1T'*a_{H+}^n$	$K_2T*a_{H+}^n$	$K_3T*a_{H+}^n$	r (mol/cm^2/s)	Log r	s(m^2/g)
0	8,40E-18	6,68E-15	3,35E-09	3,35E-09	-8,475	0,16
1	2,98E-17	6,68E-15	2,66E-10	2,66E-10	-9,5751	0,16
2	1,06E-16	6,68E-15	2,11E-11	2,11E-11	-10,675	0,16
3	3,75E-16	6,68E-15	1,68E-12	1,69E-12	-11,773	0,16
4	1,33E-15	6,68E-15	1,33E-13	1,41E-13	-12,85	0,16
5	4,72E-15	6,68E-15	1,06E-14	2,20E-14	-13,658	0,16
6	1,68E-14	6,68E-15	8,41E-16	2,43E-14	-13,615	0,16
7	5,95E-14	6,68E-15	6,68E-17	6,62E-14	-13,179	0,16
8	3,12E-13	6,68E-15	5,32E-18	3,18E-13	-12,497	0,16
9	7,49E-13	6,68E-15	4,22E-19	7,55E-13	-12,122	0,16
10	2,66E-12	6,68E-15	3,35E-20	2,66E-12	-11,575	0,16

Table 8: rate of reaction (mol/s) calculated at 75^0C for sample MiB based on eq. (2.1)

pH	$K_1T'*a_{H+}^n$	$K_2T*a_{H+}^n$	$K_3T*a_{H+}^n$	r (mol/cm^2/s)	Log r	s(m^2/g)
0	8,40E-18	6,68E-15	3,35E-09	3,35E-09	-8,475	0,51
1	2,98E-17	6,68E-15	2,66E-10	2,66E-10	-9,5751	0,51
2	1,06E-16	6,68E-15	2,11E-11	2,11E-11	-10,676	0,51
3	3,75E-16	6,68E-15	1,68E-12	1,69E-12	-11,773	0,51
4	1,33E-15	6,68E-15	1,33E-13	1,41E-13	-12,851	0,51
5	4,72E-15	6,68E-15	1,06E-14	2,20E-14	-13,658	0,51
6	1,68E-14	6,68E-15	8,41E-16	2,43E-14	-13,614	0,51
7	5,95E-14	6,68E-15	6,68E-17	6,62E-14	-13,179	0,51
8	3,12E-13	6,68E-15	5,31E-18	3,18E-13	-12,497	0,51
9	7,49E-13	6,68E-15	4,21E-19	7,56E-13	-12,122	0,51
10	2,66E-12	6,68E-15	3,35E-20	2,67E-12	-11,574	0,51

C. CALCULATING THE GEOMETRIC SURFACE AREA

$$r(cm) = \frac{1}{2d} * 10^{-4} \quad \text{..... (1)}$$

The number (Nr.) of particles was calculated for 1g of basaltic glass material.

$$Nr.particles\ per\ gram = \frac{\text{volume fraction}(cm^3)}{\text{volume of particles}(cm^3)} \quad \text{..... (2)}$$

Assuming each grain is spherical, the surface area and volume of Particles was calculated based on their radius obtained from the grain size analysis.

$$SA = 4\pi r^2 \quad \text{..... (3)}$$

$$Vol.particle\ (cm^3) = \frac{4}{3}\pi r^3 \quad \text{..... (4)}$$

The volume of fraction was determined from the volume of the basalt and Differential volume of the particles. The differential volume was obtained from the LS-PSA. Hence, a basalt density of 2.9g/cm^3 was used to calculate the Volume of 1g basalt. The Volume of basalt (total volume) was calculated by;

$$Vol.basalt(cm^3) = \frac{1\ \text{g}}{2.9\ g/cm^3} \quad \text{..... (5)}$$

Then,

$$Vol.fraction(x_i\ in\ cm^3) = Diff.Volume\% * Vol.basalt(cm^3) \quad \text{..... (6)}$$

Since the specific surface area (s) of reaction is expressed in terms of the radius and density of the particles, placing together eq. 1, 2, 3, and 4 can give us the geometric specific surface area of reaction of the particles in each sample.

$$s_{geo} = \frac{3}{\rho} \sum_i \frac{x_i}{r} \quad \text{..... (7)}$$

Where x_i, i, ρ and r are fraction of volume per gram of basaltic glass, fraction of individuals, density and radius of grains respectively.

Table 9. Specific surface area (m^2/g), Nr. of grains/gram and Volume fraction (cm^3) of each particle size calculated according to the formulas given in equation 7 above, sample MiB. All grains are assumed to be sphere

d(μm)	r(cm)	Diff. Vol%	SAP(4πr2)	Vol part.(4/3πr3)	Vbasalt(1g/ρ)	Vol. fraction	Nr.particles/g	SA fract.(m2/g)
0,474	2,37E-05	1,60	7,10E-09	5,56E-14	0,34	0,01	9,92E+10	0,07
0,755	3,78E-05	3,95	1,80E-08	2,25E-13	0,34	0,01	6,06E+10	0,11
1,204	6,02E-05	5,09	4,60E-08	9,11E-13	0,34	0,02	1,93E+10	0,09
1,919	9,60E-05	5,58	1,20E-07	3,69E-12	0,34	0,02	5,22E+09	0,06
3,06	1,53E-04	7,00	2,90E-07	1,50E-11	0,34	0,02	1,61E+09	0,05
4,878	2,44E-04	10,10	7,50E-07	6,06E-11	0,34	0,03	5,75E+08	0,04
7,776	3,89E-04	14,30	1,90E-06	2,45E-10	0,34	0,05	2,01E+08	0,04
12,4	6,20E-04	18,70	4,80E-06	9,95E-10	0,34	0,06	6,48E+07	0,03
19,76	9,88E-04	19,50	1,20E-05	4,03E-09	0,34	0,07	1,67E+07	0,02
31,51	1,58E-03	10,50	3,10E-05	1,63E-08	0,34	0,04	2,22E+06	0,01
50,23	2,51E-03	1,96	7,90E-05	6,62E-08	0,34	0,01	1,02E+05	0,00
80,07	4,00E-03	0,92	2,00E-04	2,68E-07	0,34	0,00	1,18E+04	0,00
127,7	6,39E-03	0,57	5,10E-04	1,09E-06	0,34	0,00	1,81E+03	0,00
203,3	1,02E-02	0,09	1,30E-03	4,39E-06	0,34	0,00	6,68E+01	0,00
Total								0,52

Similarly, the geometrical surface area for the hand crushed sample was found 0.16 m^2 per gram.

APPENDIX II: Mass calculation

Mole of basalt that is required to get 28kg P per hectare per year in a year at 10^0C and pH 4 for the micronized sample could be calculated;

$$x_p^b\left(n_b - n_b \exp\ (-(k * s * M_b * t)\right) = C_P\left(\frac{kg}{ha.yr}\right) \text{ .....1}$$

$$x_p^b(n_b(1 - exp^{-(k*s*M_b*t)} = C_P\left(\frac{kg}{ha.yr}\right) \text{ .....2}$$

By rearrangement,

$$n_b = \frac{C_P\left(\frac{kg}{ha.yr}\right)}{x_p^b\,(1-exp^{-(k**s*M_b*t)}} \quad \text{.....3}$$

Where n_b is moles basalt per hectare per year, x_p^b is fraction of phosphorus in the basalt, k specific rate constant (moles. $m^{-2}.s^{-1}$) at 10^0C & pH 4, s Specific surface area ($m^2.g^{-1}$) M_b moleculare mass ($g.mol^{-1}$) and t time(s).

$$n_b = \frac{904\left(\frac{moles\ P}{ha.yr}\right)}{0.004\ (1-exp^{-(1.29*10^{-10}\ *0.52\ *124.4\ *\ 3.15*10^7)}}$$

$$n_b = 976536.81\frac{mole}{ha.\,yr} = 121{,}481.2\ kg\ basalt\ per\ hactare\ per\ year$$

Similarly, mole of basalt required to obtain 140 kg K per hectare per year would be calculated as;

$$n_b = \frac{C_k\left(\frac{kg}{ha.\,yr}\right)}{x_p^b\ (1 - exp^{-(k**s*M_b*t)}} = \frac{3580.56\left(\frac{moles\ P}{ha.\,yr}\right)}{0.008\ (1 - exp^{-(1.29*10^{-10}\ *0.52\ *124.4\ *\ 3.15*10^7)}}$$

$$n_b = 1934342.1\frac{mole}{ha.\,yr} = 240{,}632.2\ kg\ basalt\ per\ hectare\ per\ year$$

APPENDIX III: Procedure of preparing solutions for second experiment

A. H_2SO_4

$$M_1 * V_1 = M_2 * V_2$$

Molarity given in the container is M_1 (95%) the density of the acid is 1, 84 g/cm^3 and the reaction volume is V_2 (300ml).

M_1= (0,95 *1840g/l) / 98g/mol **= 17.84mol/kgw**

The volume of the sulfuric acid to be added is V_1;

V_1 = (0.5M* 300)/17.84 = **8.4ml**

B. HCl

The labeled molarity M_1 is 37% and density of 1.19g/cm^3. Hence, V_1 is calculated;

$$M_1V_1 = M_2V_2$$

$$HCL = H^+ + Cl^-$$

$$((0.37*1190g/l)/36.5g/mol)* V_1 = 1M*300ml$$

V_1= 300ml/12.06 = **24.87ml** of HCl will be used to prepare 1M (1N) of HCl

C. HNO_3

$$HNO_3 = H^+ + NO_3^-$$

$M_1V_1 = M_2V_2$, where M_1 is 65% and density is 1.39g/cm^3

V_1 = 300ml.M/ ((0.65*1390)/63g/cm^3) = **20.92ml** of HNO_3 will be used to prepare the 1M of HNO_3.

APPENDIX IV: Results from the basalt acid base treatment

Table 11: Concentration Values for selected anions from the batch experiment of basalt glass reacted with nitric acid.

HNO3			
F^-(ppm)	**Cl^- (ppm)**	**SO_4^{2-} (ppm)**	**PO_4^{3-} (ppm)**
17,03	302,95	429,26	1706,60
20,19	302,30	424,42	1745,83
17,32	304,13	418,08	1741,26
17,51	302,84	411,80	1744,25
18,54	306,80	418,57	1752,21
19,98	310,41	420,89	1758,99
21,48	312,10	432,77	1756,32
26,97	307,98	424,96	1766,06
41,19	364,63	390,83	1698,42

Table 12: Concentration Values for selected anions from the batch experiment of basalt glass reacted with Hydrochloric acid. Values written as n.a. are very low to be detected.

HCl			
F^-(ppm)	**Cl^- (ppm)**	**SO_4^{2-} (ppm)**	**PO_4^{3-} (ppm)**
16,05968	90695,09	392,4127	1702,754
19,49637	61939,54	411,398	1743,969
18,99625	65937,73	421,8084	1756,747
19,03894	59402,74	415,0217	1753,785
20,06963	76929,24	425,026	1775,869
18,64604	61259,24	416,3884	1775,024
19,59055	64363,63	414,7875	1765,561
19,68539	65767,85	421,4101	1769,279

Table 13: Concentration Values for selected anions from the batch experiment of basalt glass reacted with Sulfuric acid. Values written as n.a. are very low to be detected.

H2SO4			
F^-(ppm)	**Cl^- (ppm)**	**SO_4^{2-} (ppm)**	**PO_4^{3-} (ppm)**
15,49201	303,714	116477,5	1663,518
19,41337	309,148	60869,92	1667,921
19,97416	302,1785	65611,38	n.a
19,41972	304,4354	61571,62	1711,188
19,49205	302,3125	60872,06	1707,551
20,2984	306,6387	70759,33	1718,63
20,26321	308,7862	68708,73	1710,36
20,68124	304,3348	71790,48	1722,998

APPENDIX V: Phreeqc Simulation data block

a.

```
Solution 1
-pH 1
-temp 25.0
   #H2SO4
units  ppm
Ca     16.5
Mg     12.3
Na     2.9
K      0.58
F      19.4
Cl     303.7
S(6)   60869.9
P      1711.18

REACTION 1
     NaOH    1
     2 moles in 100 steps
Selected_output
-file m:\H2SO4Psaturation25.txt
-molalities  Ca+2 Mg+2 Na+ K+ F- PO4-3
-saturation_indices O2(g)    Hydroxylapatite Fluorapatite
                             Brushite Brucite Fluorite Halite Gypsum

```

b.

```
Solution 1
-pH 1
-temp 90.0
   #H2SO4
units  ppm
Ca     16.5
Mg     12.3
Na     2.9
K      0.58
F      19.4
Cl     303.7
S(6)   60869.9
P      1711.18

REACTION 1
     NaOH    1
     2 moles in 100 steps
Selected_output
-file m:\H2SO4Psaturation25.txt
-molalities  Ca+2 Mg+2 Na+ K+ F- PO4-3
-saturation_indices O2(g)    Hydroxylapatite Fluorapatite
                             Brushite Brucite Fluorite Halite Gypsum
```

Input data block that define the Simulation reaction of the aqueous solution from $H2SO_4$ with NaOH at 25(a) and 90 ^{0}C (b)

a.

```
Solution 1
-pH 1
-temp 25.0
   #HCl
units  ppm
Ca     14.3
Mg     9.9
Na     2.8
K      0.4
F      18.6
Cl     59402.7
S(6)   415.0
P      1765.6

REACTION 1
     NaOH    1
     2 moles in 100 steps

Selected_output
-file m:\HClPsaturation25.txt
-molalities  Ca+2 Mg+2 Na+ K+ F- PO4-3
-saturation_indices O2(g)    Hydroxylapatite Fluorapatite Brushite
                             Brucite Fluorite Halite Gypsum
```

b.

```
Solution 1
-pH 1
-temp 90.0
   #HCl
units  ppm
Ca     14.3
Mg     9.9
Na     2.8
K      0.4
F      18.6
Cl     59402.7
S(6)   415.0
P      1765.6

REACTION 1
     NaOH    1
     2 moles in 100 steps

Selected_output
-file m:\HClPsaturation90.txt
-molalities  Ca+2 Mg+2 Na+ K+ F- PO4-3
-saturation_indices O2(g)    Hydroxylapatite Fluorapatite Brushite
                             Brucite Fluorite Halite Gypsum
```

b. Input data block that define the Simulation reaction of the aqueous solution from HCl with NaOH at 25(a) and 90 ^{0}C (b)

a.

```
Solution 0
-pH 1
-temp 25.0
   #HNO3
units  ppm
Ca     18.3
Mg     11.9
Na     3.1
K      0.5
F      17.5
Cl     302.8
S(6)   420.8
P      1746.3

REACTION 1
    NaOH    1
    2 moles in 100 steps

Selected_output
-file m:\HNO3 Psaturation.txt
-molalities  Ca+2 Mg+2 Na+ K+ F- PO4-3
-saturation_indices O2(g)  Hydroxylapatite Fluorapatite Brushite
                           Brucite Fluorite Halite Gypsum
```

b.

```
Solution 0
-pH 1
-temp 90.0
   #HNO3
units  ppm
Ca     18.3
Mg     11.9
Na     3.1
K      0.5
F      17.5
Cl     302.8
S(6)   420.8
P      1746.3

REACTION 1
    NaOH    1
    2 moles in 100 steps

Selected_output
-file m:\HNO3 Psaturation.txt
-molalities  Ca+2 Mg+2 Na+ K+ F- PO4-3
-saturation_indices O2(g)  Hydroxylapatite Fluorapatite Brushite
                           Brucite Fluorite Halite Gypsum
```

Input data block that define the Simulation reaction of the aqueous solution from HNO_3 with NaOH at 25(a) and 90 ^{0}C (b)